Understanding the patterned deposition of lignin in secondary cell walls

by

Eva Yi Chou

B.Sc., The University of British Columbia, 2014

A THESIS SUBMITTED IN PARTIAL FULFILLMENT OF THE REQUIREMENTS FOR THE DEGREE OF

MASTER OF SCIENCE

in

The Faculty of Graduate and Postdoctoral Studies

(Botany)

THE UNIVERSITY OF BRITISH COLUMBIA

(Vancouver)

December, 2016

Abstract

Lignin, one of the three main components of the secondary cell wall, is an important phenolic biopolymer that provides strength and rigidity to the cell walls of tracheary elements and fibers in vascular plants. Lignin is composed of phenolic alcohol monomers called monolignols, which are synthesized in the cytoplasm. These monolignols are exported to the apoplast where they polymerize by random radical coupling following oxidation by laccases and peroxidases. Two laccases found in *Arabidopsis thaliana*, LAC4 and LAC17, were localized to secondary cell wall, and required for lignification of protoxylem tracheary elements. The localization of LAC4 and LAC17 to spiral secondary cell walls could be due to either: 1) the diffuse secretion of laccases followed by remobilization to the secondary wall, or 2) a reorientation of post-Golgi vesicle trafficking to secondary cell wall specific plasma membrane domains. Localization studies with LAC4-RFP driven by a constitutive promoter found laccases localized to all regions of the primary cell wall prior to differentiation, then the localization shifted into the helical secondary cell wall bands during protoxylem tracheary elements differentiation. This change in localization suggests there is a change in vesicle traffic during secretion of secondary cell wall components (such as laccases). Furthermore, Fluorescence Recovery After Photobleaching (FRAP) was used to determine if laccase localization in secondary cell walls was due to constraint by the secondary cell walls or exclusion from the primary cell wall. Laccases were also found to be immobile in secondary cell wall domains, but mobile when expressed ectopically in primary cell wall domains. Further drug and mutant FRAP studies found laccases remain immobile in the absence of secondary cell wall: cellulose, xylan, lignin and xylan/lignin. These results suggest laccases are not only anchored to secondary cell

wall specific components but may be anchored to multiple components of the secondary cell wall or an unknown component of the secondary cell wall.

Preface

Pr35s::VND7-GR constructs (Yamaguchi *et al.,* 2010), T87 Arabidopsis cell lines (both wildtype and *VND7-GR* transformed) and *irx3-4 baculites-like1* mutants with the *VND7-GR* construct were provided by Dr. Taku Demura (Nara institute of science and technology, Nara, Japan). I transformed *irx3-4 baculites-like1/VND7-GR* plants with *prLAC4:LAC4-mCHERRY*. The *prLAC4:LAC4-mCHERRY* (Schuetz *et al.,* 2014)*, prUBQ10:LAC4-mCHERRY* and *prUBQ10:sec-mCHERRY* plant lines were provided by Dr. Mathias Schuetz and Anika Benske. *irx10/irx10-L* mutants (Brown *et al.,* 2005, 2009) transformed with *prLAC4:LAC4-mCHERRY* and the VND7-GR constructs were provided by Miranda Meents and Dr. Mathias Schuetz (Samuels Lab, unpublished). The *35S:sec-mCITRINE* (DeBono *et al*., 2009) constructs I used for cloning *prCESA7:sec-mCITRINE* were plant lines from our lab made by Dr. Allen DeBono and the pKGK-prCESA7 Gateway vector and sequencing primers were designed by Dr. Mathias Schuetz.

In chapter 3, the time-course experiments done with *prLAC4:LAC4-mCHERRY* plant lines to track laccases were done by Dr. Mathias Schuetz. I imaged all other fluorescence micrographs and the *prUBQ10:sec-mCHERRY* timecourse. T87 Arabidopsis cell line Co-IP was done by me with the assistance of Dr. Yoshito Ogawa and the mass spectrometry data was generated by Ms. Rei Kurata at the Nara institute of science and technology (Nara, Japan).

The micrographs, FRAP images, recovery curves and statistics in chapter 4 were imaged and analyzed by me.

Table of Contents

List of Tables

List of Figures

List of Abbreviations

Abbreviation	Full name
1CW	Primary cell wall
2CW	Secondary cell wall
ABC	ATP binding cassette
CASP1	Casparian Strip Domain Protein1
CesA	Cellulose synthase
COG2	Conserved Oligomeric Golgi 2
CSC	Cellulose synthase complex
DCB	2,6-dichlorobenzonitrile
E. coli	Escherichia coli
ER	Endoplasmic reticulum
F_m	Mobile fraction
FRAP	Fluorescence recovery after photobleaching
G	Guaiacyl
G-lignin	coniferyl alcohol
GM	Germination media
GR	gluticorticoid receptor
H	Hydroxy phenol
H-lignin	p-coumaryl alcohol
irx	Irregular xylem
LB	Luria Bertani
LS	Linsmaier and Skoog
MAP	Microtubule-associated proteins
MS	Murashige and Skoog
PA	Piperonylic acid
PCD	programmed cell death
RFP	Red fluorescent protein
RT	Room temperature
ROI	Region of interest
S	Syringyl
S-lignin	sinapyl alcohol
SD	Standard deviation
T½	Half time of fluorescence recovery
TE	tracheary element
TEM	transmission electron microscopy
TGN	trans-Golgi network
VETH1	Vesicle Tethering 1

VETH2	Vesicle Tethering 2
VND6	VASCULAR-RELATED NAC-DOMAIN6
VND7	Vascular-Related NAC-Domain 7
VND7	VASCULAR-RELATED NAC-DOMAIN7
YFP	Yellow fluorescent protein

Acknowledgements

I would like to sincerely thank my supervisor, Dr. Lacey Samuels for her mentorship, support and patience over the course of these two years. I am extremely grateful to her for this learning opportunity. I would also like to thank my supervisory committee members, Dr. George Haughn and Dr. Abel Rosado for their guidance and advice.

This project could not be accomplished without the mentorship of Dr. Mathias Schuetz who has been a great research mentor, is always available for questions and has been indispensable in my learning of cloning techniques. He and Yoichiro Watanabe have both spent endless hours teaching and training me on fluorescence microscopy and micrograph editing techniques and I would like to extend my thanks to both of them. I would also like to thank Dr. Teagen Quilichini and Miranda Meents for their guidance on electron microscopy techniques and all members of the Samuels lab for all their support.

I am also thankful to members of the Demura lab at the Nara Institute of Science and Technology (especially Dr. Taku Demura, Dr. Yoshito Ogawa, Dr. Misato Ohtani, Dr. Yuto Takanaka and Ms. Rei Kurata) for their assistance in teaching co-immunoprecipitation as well as hosting me in Nara, Japan for three weeks.

I am grateful to the Botany department staff and fellow grad students for their assistance and encouragement. I would like to thank the UBC Bioimaging facility for their assistance and training on the spinning disc confocal and electron microscope.

I am also forever grateful to my family, friends, and church group (especially my savior, Jesus Christ) for their support and encouragement.

Chapter 1: Introduction

1.1 Overview

This thesis explores how xylem cells develop their strong, lignified secondary cell wall. Previous studies demonstrated that oxidative enzymes (laccases) are required for lignin to be polymerized in the wall, and laccases are deposited in patterns that correspond exactly to secondary, but not primary, cell wall domains. The goal of my thesis work was to understand laccase secretion and localization in the secondary cell wall. I hypothesized that the patterned deposition of laccases seen in protoxylem tracheary elements may be due to a reorientation in secretory vesicle flow during xylem differentiation. Further, I tested the hypothesis that the laccase protein was constrained to specialized domains post-secretion by anchoring to polysaccharide or lignin components of the secondary cell wall.

1.2 Plant cell walls

Plant cells have a strong extracellular matrix composed of polysaccharides and proteins. This extracellular matrix, known as the plant cell wall, plays important roles in the plant's defense, development, and transport of water and nutrients (Cosgrove, 2005). While plant cells are typically surrounded by a primary cell wall (1CW), some specialized cell types such as tracheary elements and fibers deposit a secondary cell wall (2CW) after cellular elongation (Fukuda, 1996). These 2CWs are essential for water/nutrient transport and provide structural support (Fukuda, 1996). The evolution of 2CW gave plants the ability to colonize land and to grow to astounding heights (Zhong and Ye, 2015; Raven *et al.,* 2005).

The plant cell walls are not only important in providing the plant structure with strength and rigidity, they are important in a number of industries as well (Ragauskas *et al.,* 2014). 2CW-rich biomass, such as wood, plays a large role in the construction, and pulp and paper industries. The cellulose found in the 2CWs are important to the textile and biofuel industries. Important lignin products include polymeric membrane, thermoplastic elastomers and low-cost carbon fibers (Ragauskas *et al.,* 2014).

1.2.1 Primary and secondary cell walls

Plant 1CWs are composed primarily of three components: cellulose, hemicellulose and pectin (Albersheim *et al.,* 2010). This tough but flexible, gel-like matrix provides both mechanical and structural support while allowing the cells to still expand and grow (Cosgrove, 2005). Embedded in a pectin-hemicellulose matrix, the cellulose microfibrils are composed of liner β (1-4) glucan chains, and cellulose is the world's most abundant biopolymer (McFarlane, *et al*., 2014). These cellulose microfibrils are synthesized at the plasma membrane by cellulose synthase complexes (CSCs). Using UDP-glucose, the CSCs synthesize and extrude the cellulose microfibrils in the developing cell wall (Liepman *et al.,* 2010; McFarlane *et al.,* 2014). While cellulose is synthesized at the plasma membrane, the 1CW pectin and hemicellulose are made in the Golgi before being secreted to the cell wall via post-Golgi mediated vesicles (Cosgrove, 2005).

In addition to the 1CW, some specialized cell types, such as the plant fibers and tracheary elements, also have a 2CW deposited after cell maturity (Fukuda, 1996). Like the 1CWs, the 2CWs also contain cellulose microfibrils composed of liner β (1-4) glucan chains

(Albersheim *et al.,* 2010). Though different cellulose synthases (CesAs) make the CSCs, the 2CW cellulose are also made at the plasma membrane by CSCs (Watanabe *et al.,* 2015).

The 2CW contains specific hemicelluloses with β (1-4) linked mannose, and xylose polysaccharides backbones (Albersheim *et al.,* 2010). In eudicots, the major hemicellulose in 2CWs is glucoronoxylan (xylan) consisting of β (1-4) linked xylose backbone with glucuronic acid, acetyl and 4-O- methylglucuronic acid side chains (Rennie and Scheller, 2014). Glucoronoxylan has been proposed to interact with other polymers within the cell wall by crosslinking cellulose microfibrils together through hydrogen bonds as well as covalently binding to lignin through ester bonds via the glucuronic acid side chains (Busse-Wicher *et al.,* 2016; Rennie and Scheller, 2014; Watanabe and Koshijima, 1988). Xylan biosynthesis occurs within the Golgi apparatus, and xylans are subsequently secreted to the cell wall by secretory vesicles (Rennie and Scheller, 2014).

The third main component of 2CWs is the phenolic biopolymer, lignin (Albersheim *et al.,* 2010). Lignin is a cross-linked polymer formed from phenolic alcohol precursors called monolignols. There are three main types of lignin units, hydroxy phenol (H), guaiacyl (G) and syringyl (S), which polymerize from the corresponding monolignols: p-coumaryl alcohol (H-lignin), coniferyl alcohol (G-lignin), and sinapyl alcohol (S-lignin). These monolignols are synthesized in the cytoplasm before being transferred to the apoplast (Zhong and Ye, 2015). From there, the monolignols are polymerized into lignin following oxidation by peroxidases or laccases (Vanholme *et al.,* 2010). Further details on peroxidase and laccase oxidative coupling in lignin formation can be found in chapter 1.2.2 below.

1.2.2 Golgi-related secondary cell wall polysaccharide synthesis

While the lignin precursors, monolignols, and related oxidative enzymes are synthesized in the cytoplasm and ER, the major 2CW hemicellulose, xylan, is synthesized in the Golgi. Xylan synthesis begins with the conversion of UDP-glucuronic acid to UDP-xylose (Rennie and Scheller, 2014). Both Golgi and cytosolic UDP-glucuronic acid decarboxylase is involved in this conversion and any UDP-xylose synthesized in the cytosol is brought into the Golgi via UDP-xylose transporters (Kuang *et al.,* 2016; Rennie and Scheller, 2014).

The xylose backbone of xylan is assembled in the Golgi. Analysis of mutant glycosyltransferase genes *IRX9, IRX9-like (IRX9-L), IRX10, IRX10-L, IRX14*, and *IRX14-L* reveal the xylan content to be reduced, vessels with irregular shapes (irregular xylem (*irx*) phenotype), and a decrease in xylosyltransferase activity. These studies indicate that IRX9/10/14 and their related genes act as xylosyltransferases involved in the synthesis of the xylose backbone (Brown *et al.,* 2007; Lee *et al.,* 2007; Brown *et al.,* 2009; Wu *et al.,* 2009; Wu *et al.,* 2010). In dicots, the xylan backbone is further decorated by glucuronic acid by GUX1/2, Acetyl groups by RWA, and 4-O- methylglucuronic acid (GXMT1) side chains (Rennie and Scheller, 2014).

After being synthesized/modified in the Golgi, xylan is packaged into secretory vesicles at the trans-Golgi network (TGN). It is currently uncertain if cell wall polysaccharides are packaged together or independently of cell wall proteins (such as laccases). Studies using fluorescence microscopy and transmission electron microscopy (TEM) on seed coat in a TGN protein mutant (*echidna*) reveals mistargeting of both cell wall polysaccharides and proteins (McFarlane *et al.,* 2013). While both polysaccharides and proteins were found to be

mislocalized, polysaccharides were found to accumulate in the vacuole, post-Golgi secretory vesicles and endoplasmic reticulum (ER)-bodies while proteins instead accumulated in multilamellar-bodies (McFarlane *et al.,* 2013). This difference in mistargeting between polysaccharides and proteins suggests the two cell wall components may be packaged and secreted independently during 2CW formation.

1.2.2 Xylem tracheary element differentiation and secondary cell wall pattern deposition

2CWs are mainly found in the tracheary element (TE) and fiber cells of the plant vascular tissue system. In this thesis, I studied protoxylem vessels, a specific type of TE that develops in young, rapidly expanding plant organs. TEs arise from mitosis in primary meristems; they undergo elongative growth, and acquire a procambium cell fate. Once they have fully elongated, 2CWs are deposited in spiral or helical patterns underneath the 1CW. Once the 2CWs are laid down, cells undergo programmed cell death (PCD) to form a hollow skeleton of cell walls. These hollowed TEs are joined to similar axial neighbors through modification of the cell walls that connect them. These modifications are done by cell wall degrading enzymes (such as cellulases and pectinases), which cause the formation of perforation plates between the adjacent cells to form hollow tubes which, due to strengthening by the 2CWs, are able to withstand the negative pressure of water/solute transport (Turner *et al.,* 2007). The helical or spiral 2CW patterns allow the xylem TE cell to maintain an open water passage while the TE is passively elongated by the active elongation of surrounding cells.

Unlike protoxylem TEs, metaxylem TEs are deposited once elongation ceases, and they make up the majority of vessel elements in the primary vascular system. Metaxylem vessels follow the same series of developmental steps outlined for protoxylem TE above, i.e. growth

and primary wall deposition, procambial cell fate, secondary cell wall deposition, and programmed cell death. However, the 2CW of metaxylem TEs are laid down in reticulate or pitted patterns, due to different cytoskeletal arrays that differ from that of protoxylem TE. The plant cell cytoskeleton plays an important role in the patterning of the 2CWs in xylem tissues. Disruption of actin with lantrunculin B causes Golgi containing CSCs to cease movement, resulting in the loss of the usual cellulose synthase complex banding pattern on the plasma membrane of protoxylem TE (Wightman and Turner, 2008). Bundles of cortical microtubules have been shown to be closely associated with plasma membrane adjacent to developing 2CW domains in protoxylem TE (Hepler and Newcomb 1964), and disruption of these domains with microtubule inhibitors causes not only a loss of the organized CSC banding pattern at the plasma membrane but also a disruption of 2CW banding pattern (Watanabe *et al.,* 2015; Wightman and Turner, 2008). Microtubule-associated proteins (MAPs) were also demonstrated to be important in 2CW patterning in metaxylem vessels. One such MAP, MIDD1, is involved in the formation of 2CW pits in metaxylem TE cells through depolymerisation of microtubules (Oda and Fukuda, 2012). It is presently not clear what mechanisms control the restriction of MT to the regions of plasma membrane that underlie the spiral 2CW domains of protoxylem TE.

The non-cellulose components of the 2CW are made in, or transit through the Golgi, before targeted secretion to 2CW, but not 1CW domains (Schuetz *et al.,* 2014). Recent research by Oda *et al.* (2014) suggests that cortical microtubules interact with secretory vesicle targeting components, such as the exocyst complex via the Vesicle Tethering 1 and 2 (VETH1 and VETH2) and Conserved Oligomeric Golgi 2 (COG2) proteins. The VETH-COG2 complex was

shown to tether the exocyst subunit, EXO70A1, to the cortical microtubule (Oda *et al*., 2014). *EXO70A1* is preferentially expressed in xylem tissues, and loss of function mutations leads to altered 2CW patterns, presumably due to mistargeting of post-Golgi vesicles carrying xylan and CSC (Li *et al.,* 2010). Taken together, these finding suggest EXO70A1 is responsible for the recruitment of secretory vesicles to the cortical microtubules.

It has been difficult to understand the complexity of interplay between the cytoskeleton, cellulose synthases in the plasma membrane, and endomembrane system during the deposition of annular or helical 2CWs in the protoxylem TE, because the cells are deep within the plant organs. However, new studies on transcriptional regulation of xylem cells have produced new ways to study TE differentiation.

1.2.3 Transcriptional regulation of xylem TE differentiation

To understand the genetic control of 2CW biosynthesis, microarray analysis was performed on protoxylem TE-induced Arabidopsis suspension cell cultures (Demura *et al*., 2002). Two transcription factors involved in the regulation of TE cell fate (*VASCULAR-RELATED NAC-DOMAIN6* (*VND6*) and *VND7)* were identified (Kubo *et al*., 2005*).* In this study, repression of VND6 expression lead to a decrease in metaxylem TEs formation while repression in VND7 resulted in a loss of protoxylem TEs. When overexpressed, VND6 overexpression lines displayed ectopic formation of metaxylem TE cells while VND7 overexpression resulted in ectopic differentiation of protoxylem TEs (Kubo *et al*., 2005). These transcription factors have been shown to be master regulators in initiating TE differentiation (Kubo *et al*., 2005; Yamaguchi *et al*., 2010; Yamaguchi *et al*., 2011).

Discovery of the transcriptional switches for initiating TE cell fate allowed its development of experimental tools to studying xylem development, including 2CW formation. Due to TE differentiation ending in PCD, constitutive expression of plants expressing the VND7 gene leads to cell death, therefore an inducible system was developed for ectopic VND7 expression by Yamaguchi *et al*. (2010). Both the activation domain of herpes virus VP16 and the hormone-binding domain of a rat glucocorticoid receptor (GR; Aoyoma and Chua, 1997) were fused to the C terminus of VND7 (VND7-GR) (Yamaguchi *et al*., 2010). When VND7-GR is expressed in plants with the constitutive promoter 35S, as with mammalian GR (Hayashi *et al*., 2004), the glucocorticoid receptor domain is believed to bind endogenous heat-shock proteins to trap the VND7-GR in the cytoplasm. When the synthetic glucocorticoid, dexamethasone, is added, the VND7 transcription factor is freed from the heat-shock protein, allowing VND7 to enter the nucleus and initiate transcription of downstream genes (Yamaguchi *et al.,* 2010). VND7 target genes include the biosynthetic enzymes for 2CW components: cellulose, lignin and xylan (Yamaguchi *et al.,* 2011). This inducible system has been used to study cellulose biosynthesis (Watanabe *et al.,* 2015), xylan biosynthesis (Meents, unpublished data); and lignin deposition (Schuetz *et al.,* 2014) in the induced protoxylem TEs.

1.3 Lignin

1.3.1 Monolignol biosynthesis and export

Monolignols are synthesized from phenylalanine through the general phenylpropanoid and monolignol biosynthetic pathways (Whetton and Sederoff, 1995; Boerjan *et al.,* 2003). This synthesis occurs in the cytoplasm associated with ER membranes (Vanholme *et al.,* 2010). After synthesis, monolignols are translocated to the cell wall (Sibout and Hofte, 2012). Several

different models of monolignol export out of the cell have been proposed and passive diffusion, or active transport, facilitated by ATP binding cassette (ABC) transporters, may be involved (Liu *et al.,* 2011). Using the inducible VND7-GR system, Schuetz *et al.* (2014) localized candidate ABC transporters putatively involved in monolignol transport (ABCG11, ABCG29, ABCG33) to the plasma membrane. All ABC transporters were equally distributed across the plasma membrane adjacent to both the 1CW and the 2CW regions. Enzymes involved in the biosynthesis of monolignols were also evenly distributed throughout the cytoplasm (Schuetz *et al.,* 2014). This suggests monolignols are not synthesized and exported in a polar manner to the 2CW domains.

1.3.2 Oxidative coupling of monolignols

Lignin is formed through the random coupling of monolignol radicals. Monolignols are converted to monolignol radicals by oxidative enzymes of the peroxidase and laccase families (Pandey *et al.,* 2016). Radicals are usually formed on the β side chain of monolignols and these radicals are randomly coupled with the radical of another monolignol, forming different covalent bonds between the units (the most common of which are β-O-4, β -5 and β - β). This process repeats, building the stable biopolymer, lignin (Strong and Claus 2011; Marjamaa *et al.,* 2009; Ralph *et al.,* 2004; Boerjan *et al.,* 2003).

Peroxidases are iron containing enzymes that use hydrogen peroxide to produce substrate radicalization (Marjamaa *et al.,* 2009). In Arabidopsis there are 73 peroxidase genes predicted in the genome (Welinder *et al.,* 2002). Peroxidases have been shown to be required for the plant Casparian strip lignification and are recruited there by Casparian Strip Domain Protein1 (CASP1) (Lee *et al.,* 2013).

The Arabidopsis laccase family consists of 17 genes (Turlapati *et al*., 2011). Laccases contain a ring of multi-copper oxidizing centers and use oxygen to donate electrons to form the monolignol radical (Strong and Claus 2011). As the role of lignin-forming laccases in the secondary cell wall of protoxylem TE is the subject of this thesis, they are discussed more extensively in the next section.

1.4 Laccases

First discovered in plants in 1883, laccases are multi-copper containing oxidative enzymes that are heavily glycosylated, and they are predicted to contain both N and O-glycosylation sites (Strong and Claus 2011; Turlapati *et al.,* 2011). For years, there was debate about whether laccases or peroxidases were most important in oxidizing monolignols during lignification. Laccases were initially discredited due to *in vitro* studies, thus focus on monolignol polymerization fell to peroxidases (O'Malley *et al.,* 1993). Later, interest in laccases as a candidate for monolignol oxidation for lignification was revived when Sterjiades *et al.* (1992) showed monolignols could be cross-linked using laccases purified from *Acer pseudoplantanus* and Driouich *et al.* (1992) localized laccases in stems to 2CW using immunolocalization transmission electron micrographs.

Laccases have since been shown to be important to monolignol oxidation during developmental lignification through a number of studies. Microarray data of the plants induced to form protoxylem TE with the VND7-GR system, showed two Arabidopsis laccases, LAC4 and LAC17, are highly upregulated, suggesting laccases are involved in protoxylem TE differentiation (Yamaguchi *et al.,* 2011). Berthet *et al.* (2011) demonstrated the role of these laccases in Arabidopsis stem lignification through mutant *lac4/lac17* studies. Cross-sections of stems in

lac4/lac7 double mutants show xylem vessels were collapsed and no longer able to withstand the negative pressure of water transport. The lignin content of these double mutants was also found to be decreased (Berthet *et al.,* 2011). Further studies by Zhao *et al.* (2013) using triple *lac4/lac17/lac11* Arabidopsis mutants demonstrated that lack of these laccases cause plants to be extremely dwarf and the anthers of these plants to no longer dehisce. Despite peroxidase transcript levels being expressed at normal levels, the number of lignified cells in the triple *lac4/lac17/lac11* mutants were shown to be greatly decreased in both the root and the stem (Zhao *et al.,* 2013).

1.5 Secretion of laccases to the secondary cell wall

Despite these advances in our understanding of laccase function in activating monolignols during lignin polymerization, the mechanisms behind deposition of laccases into developing 2CWs are still poorly understood. In the inducible VND7-GR protoxylem TE system in *Arabidopsis thaliana,* the laccases LAC4 and LAC17 localize to 2CW domains and are responsible for the helical deposition of lignin in protoxylem TEs (Scheutz *et al.,* 2014). Unlike wild-type 2CW, when fluorescently tagged monolignols were introduced into *lac4/lac17* double mutants none of the fluorescent monolignols were incorporated into the 2CW of mutant protoxylem TE (Schuetz *et al.,* 2014). When the fluorescently tagged monolignols were introduced into plants overexpressing *LAC4* or *LAC17* lines, all cell wall domains (primary and secondary) had incorporation of the fluorescent monolignols (Schuetz *et al.,* 2014). When red fluorescent protein (mCherry) tagged LAC4 or LAC17 was expressed in the *lac4 lac17* double mutant, driven by its native promoter (e.g. *proLAC4:LAC4-mCHERRY)*, the collapsed xylem phenotype was rescued, indicating that the LAC4-mCHERRY was functional. LAC4-mCHERRY

was localized to 2CW domains specifically, but it was not found between the bands of 2CW in 1CW domains (Schuetz *et al.,* 2014). These lines of evidence suggest that laccases are found in the 2CW where lignin is deposited, they are necessary for the lignification of monolignols in 2CWs of protoxylem tracheary elements, as well as sufficient to trigger lignification in the presence of monolignols.

1.6 Research objectives

In *Arabidopsis thaliana* protoxylem TE, laccases were demonstrated to play an important role in the polymerization of monolignols to lignin. Microarray data on VND7-GR plants show LAC4 and LAC17 to be highly upregulated. In *lac4/lac17/lac11* triple mutants, lignin was shown to be abolished from the roots while *lac4/lac17* mutants have collapsed metaxylem TEs in the stems. Monolignols in *lac4/lac17* mutants were also shown to no longer polymerize to lignin in 2CW domains. Localization studies on LAC4 and LAC17 show laccases localize to 2CW domains and are responsible for the helical deposition of lignin in protoxylem TEs. These laccases were not found in 1CW domains and are specific to the 2CW domain.

Despite the current knowledge on laccase function and importance, little is known about the mechanism behind laccase secretion. While it is predicted that laccases are secreted to the apoplast of the cell via the endomembrane system, and that vesicles containing 2CW components are docked at 2CW domains rich in cortical microtubules and the exocyst complex, we still do not know if there is a change in vesicle traffic pattern during 2CW formation or how laccases are packaged at the TGN. They might be packaged into secretory vesicles with other 2CW cargo such as the dominant hemicellulose xylan, or in a different subset of secretory vesicles. Furthermore, while the localization pattern of laccases is shown to be in the 2CW only, the mechanism which keeps the laccases in the 2CW domains remains to be explored. To further explore the trafficking and packaging of laccases as well as the means by which laccases stay within the 2CW domains, I had the following research objectives:

1) **Ascertain if the secretion of extracellular proteins, such as laccases, changes during the formation of 2CWs (Chapter 3).**
2) **Test the hypothesis that the hemicellulose xylan and laccases might be cross-linked during 2CW production. (Chapter 3)**
3) **Elucidate what keeps laccases restricted to 2CW-specific domains (Chapter 4)**

Confocal microscopy will be used to complete objectives 1 and 3 above. The VND7-GR system was used due to its ability to induce the differentiation of ectopic protoxylem TEs on the epidermis of Arabidopsis seedlings where they can be easily imaged. This bypasses the issues that the native protoxylem TEs are buried deep within layers of epidermis and cortex cells, making imaging of native protoxylem TEs difficult.

To image the trafficking of laccases, fluorescently tagged laccases driven by both a native (*proLAC4:LAC4-mCHERRY*) and constitutive promoter (*proUBQ10:LAC4-mCHERRY*) were used (Schuetz *et al.,* 2014; Benske, UBC Botany M.Sc. thesis 2014) together with the VND7-GR system. To observe if a change in trafficking occurred during 2CW formation, plants with the VND7-GR system and secreted fluorescent proteins driven by either a constitutive promoter (*proUBQ10:sec-mCHERRY*) or a novel 2CW specific reporter (*proCESA7:sec-CITRINE*) were constructed to visualize trafficking patterns during 2CW formation. To test if the laccases are linked to xylans, co-immunoprecipitation experiments were performed using both VND7-GR Arabidopsis seedlings and cell cultures lines, using antibodies against either the xylan or RFP on the laccase.

Fluorescence Recovery After Photobleaching (FRAP) microscopy was used to better understand the mobility of laccases as well as to determine what components of the cell wall keep laccases in 2CW domains.

Chapter 2: Materials and methods

2.1 Plant material and growth conditions

The organism used for this study is *Arabidopsis thaliana,* Columbia-0 ecotype. *prLAC4:LAC4-mCHERRY, prUBQ10:LAC4-mCHERRY* and *prUBQ10:sec-mCHERRY* plant lines were generously provided by Dr. Mathias Schuetz and Anika Benske (Schuetz *et al.,* 2014). The *irx10/irx10-L* mutants (Brown *et al.,* 2005, 2009) transformed with *pUBQ10:VND7-GR* (Yamaguchi *et al.,* 2010) and *prLAC4:LAC4-mCHERRY* were provided by Miranda Meents and Dr. Mathias Schuetz respectively (Samuels lab, unpublished). *VND7-GR* and *irx3-4 baculites-like 1* (*cesa7*) mutant seeds were kindly provided by Dr. Taku Demura (Yamaguchi *et al.,* 2010; Takanaka *et al., New Phytologist*, in revision).

Seeds were sterilized using either chlorine gas or ethanol and germinated on germination media (GM; (1× Murashige-Skoog (MS), 1% Sucrose, 1x Gamborg's Vitamin mix, 0.05% MES at pH 5.8) and 0.75% (w/v) agar. If transgenic seed lines were not homozygous, seeds were grown on selection GM containing the appropriate antibiotics until antibiotic resistant seedlings could be discerned from non-resistant seedlings (7-14 days). Antibiotics used for this study were kanamycin (50µg/mL), hygromycin (25µg/mL) or Basta (35µg/mL). The seeds were vernalized for 24 h at 4 °C. For growth on soil, seeds were transferred to 21 °C under 24-hour light (full spectrum fluorescence illumination at 75-125 µmol/m^2S) for 7-10 days before being transferred onto soil (Sungro Sunshine Mix 4). Seedlings on soil were grown at 21 °C in 18-hour light cycles (full spectrum fluorescence illumination at 230 µmol/m^2S). For imaging, seeds were dark-grown at 21 °C for 3-5 days.

2.2 Plant DNA extraction

Plant genomic DNA was extracted from young rosette leaves of *Arabidopsis thaliana*. Two-three young rosette leaves were ground in extraction buffer (200mM tris-HCl; pH7.5, 250mM NaCl, 25mM Na_2EDTA, 0.5% SDS) and pelleted. The cell debris pellet was removed, the DNA precipitated from the solution using isopropanol and pelleted. The pelleted DNA precipitate was then washed with 70% ETOH. After allowing the precipitate to air dry, TE buffer (10mM tris-HCl; pH8.0, 1mM Na_2EDTA) was used to resuspend the DNA. Extracts were stored at -20 °C.

2.3 Cloning *proCESA7:sec-YFP*

Using the KAPA HiFi Hotstart ReadyMix® (Kapa Biosystems™), the *sec-CITRINE* gene sequence was amplified from genomic DNA of *Arabidopsis thaliana* plants containing *35S:Sec-CITRINE* (DeBono *et al*, 2009). Flanking primers used to amplify the *sec-CITRINE* gene sequences and add Invitrogen™ Gateway® attB adaptors are listed in table 1.1 below. Amplified products were gel purified using the Macherey-Nagel™ Nucleospin® Gel Clean-up Kit. Purified products were confirmed to be *sec-CITRINE* using both restriction digest (NEB: BamHI+SalI, PstI+SalI) and sequencing using the Thermofischer Scientific™ BigDye® Terminator v3.1. DNA product sequencing was done by the UBC Nucleic Acid Protein Service Unit.

Sec-CITRINE with attB adaptors fragments were cloned into the Invitrogen™ Gateway® *pDONR/Zeo* vector using Invitrogen™ Gateway® BP cloning technology. These vectors were subsequently transformed into Invitrogen™ One Shot® TOP10 Chemically Competent *Escherichia coli* (*E. coli*) using the heat-shock method. Transformed *E. coli* were grown on Luria

Bertani (LB) broth agar (0.75%) containing zeocin (50µg/mL) overnight at 37 °C. Resistant colonies were selected and propagated in liquid LB broth containing zerocin. Vectors were purified using the Qiagen™ QIAprep Spin Miniprep® Kit and sequenced using

Successful *pDONR* candidates containing *sec-CITRINE* were then used in following Gateway® LR cloning reactions using the *pKGW PrCESA7* vector (Schuetz, unpublished). Reactions were transformed into One Shot® TOP10 Chemically Competent *E. coli* using the heat-shock method. Transformed *E. coli* were grown on LB agar plates containing spectinomycin (100µg/mL) overnight at 37 °C. Resistant colonies were picked, propagated in liquid LB broth containing spectinomycin and purified using the Qiagen™ QIAprep Spin Miniprep® Kit. Purified vectors were sequenced using the Thermofischer Scientific™ BigDye® Terminator v3.1. and M13 Forward (-20) primer.

Table 1.1: Primers used for amplification of *sec-CITRINE*. Gateway attB adapters are underlined (designed by Schuetz).

Primer Name	**Sequence (5' --> 3')**
SecCitrine AttB1+F	GGGGACAAGTTTGTACAAAAAAGCAGGCT TGATAATGAAGGGTCTTCATCTCC
SecCitrine AttB2+R	GGGGACCACTTTGTACAAGAAAGCTGGGT TTATGGCGCAGCAGCACCAGCA

2.4 Transforming *Arabidopsis thaliana*

All *Arabidopsis thaliana* transformations were done using the floral dip method with *Agrobacterium tumefaciens* (Clough and Bent, 1998). Vectors generated for transformations were generated using Invitrogen™ Gateway® cloning technology.

2.4.1 Transforming the construct into *Escherichia coli*

Desired vectors to be transformed into Arabidopsis were first transformed into One Shot® TOP10 Chemically Competent *E. coli* (Invitrogen™). The *E. coli* were incubated with the vector, heat shocked at 42 °C then allowed to recover on ice. After recovery, the *E. coli* were transferred to liquid LB media and incubated at 200 rpm for 1 h at 37 °C. Following incubation, *E. coli* were cultured on LB broth agar (0.75%) plates containing antibiotics for approximately 16 h at 37 °C. Independent, resistant colonies were selected and the vector isolated. Antibiotics used for this study were kanamycin (50µg/mL), hygromycin (25µg/mL), zeocin (50µg/mL) or spectinomycin (100µg/mL).

2.4.2 Transforming the construct into *Agrobacterium tumefaciens*

Agrobacterium tumefaciens strain GV3010 was transformed with the desired vector through electroporation and immediate transfer to pre-cooled liquid LB media. Agrobacterium were subsequently incubated on a shaker (200 rpm) at 30 °C for a 4-6 h. Cultures were then removed from incubation and spread on antibiotic containing LB agar (0.75%) plates and incubated for 36-48 h at 30 °C. Independent, resistant colonies were selected for use in Arabidopsis transformations. For Agrobacterium selection LB agar plates containing a minimum

of gentamicin (50µg/mL) plus one other antibiotic (kanamycin (50µg/mL), hygromycin (25µg/mL), or spectinomycin (100µg/mL)) were used.

2.4.3 Transforming the construct into *Arabidopsis thaliana*

Antibiotic resistant *Agrobacterium tumefaciens* transformed with the desired vector were selected and cultured in liquid LB containing antibiotics for 40 h at 200 rpm at 30 °C. After 40 h, cultures were transferred to fresh liquid LB media and incubated at 200 rpm at 30 °C for 6-8 h. Silwet L-77® (GE Silicones™) was added to the cultures and Arabidopsis plants with young flowers (approximately 3 weeks old) were dipped using the floral dip method (Clough and Bent, 1998). Plants were allowed to rest in the dark at RT overnight in a humid space before being returned to growth chambers.

2.5 Generating prUBQ10:sec-mCHERRY/prCESA7:sec-YFP/*VND7-GR* plant lines

prCESA7:sec-YFP Arabidopsis plants were crossed with *prUBQ10:sec-mCHERRY/VND7-GR* plants. Successful crosses were grown on GM plates containing both kanamycin (50µg/mL) and hygromycin (25µg/mL) selection antibiotics. Resistant seedlings were transferred to soil and the F2 seeds collected for further screening.

2.5.1 Screening prUBQ10:sec-mCHERRY/prCESA7:sec-CITRINE/*VND7-GR* plant lines

3-5 day old dark grown *prUBQ10:sec-mCHERRY/prCESA7:sec-CITRINE/VND7-GR* F2 seedlings grown on GM agar plates (0.75%) were induced with dexamethasone for 36 h and imaged using an epifluorescence microscope. The presence of the yellow fluorescent protein (YFP,mCITRINE) was confirmed using an excitation filter at 450-490 nm (emission filter at 510

nm while red fluorescent protein (RFP) presence was confirmed using an excitation filter at 560/40 nm (emission filter at 595 nm). Successful differentiation of ectopic protoxylem tracheary elements were determined using brightfield microscopy by looking for 2CW spirals.

2.6 Generating *cesa7* mutant lines with both *prLAC4:LAC4-mCHERRY* and *VND7-GR* constructs

Homozygous Arabidopsis *irx3-4 baculites-like 1* (*cesa7*)/*VND7-GR* mutants (Takanaka *et al., New Phytologist*, in revision) were grown on soil until the first flowers began to open. Using the floral dip method described above, the *prLAC4:LAC4-mCHERRY* vector was transformed into the Arabidopsis plants. T1 seeds were plated on GM agar plates containing both kanamycin (50µg/mL) and hygromycin (25µg/mL) selection antibiotics. Resistant seedlings were transferred to soil and the T2 seeds collected for further screening.

2.6.1 Screening *prLAC4:LAC4-mCHERRY* and *VND7-GR cesa7* mutant plant lines

T2 seeds containing *cesa7* mutants with *VND7-GR* and prLAC4:LAC4-mCHERRY were dark grown on selection media (as above) for 3-5 days and subsequently treated with dexamethasone for 36 h. Screening for RFP presence was done using an epifluorescence microscope with a filter cube which had an excitation filter at 560/40 nm (emission filter at 595 nm). Successful differentiation of ectopic protoxylem tracheary elements were determined using brightfield microscopy by looking for 2CW spirals.

2.7 Inducing *VND7-GR* plant lines

3-5 day old etiolated *VND7-GR* seedlings (Yamaguchi *et al.,* 2010) grown on GM agar (0.75%) plates were transferred to either fresh GM agar plates or 24 well culture plates containing liquid ½ MS. Following transfer, seedlings were submerged in 10µM dexamethasone and incubated in the dark at 21 °C for 18-36 h, depending on the goals of the experiment. Lines containing *VND7-GR* (*prLAC4:LAC4-mCHERRY, prUBQ10:LAC4-mCHERRY* and *prUBQ10:sec-mCHERRY*, *cesa7* mutants, and irx10/10-L mutants) were treated in the same manner. Col-0 wild-type ecotype Arabidopsis seedlings were treated as above for comparison with induced lines.

2.8 Drug treatments

3-5 day old Arabidopsis seedlings were treated with either a piperonylic acid (PA) (Kaneda *et al.,* 2008; Chong *et al.,* 2001) or 2,6-dichlorobenzonitrile (DCB) (Meyer *et al.,* 1978) to inhibit lignin and cellulose respectively.

2.8.1 Treating plant lines with piperonylic acid

prLAC4:LAC4-mCHERRY and *prUBQ10:sec-mCHERRY* seeds were dark-grown for 3-5 days on GM agar (0.75%) plates and transferred to 24 well culture plates containing ½ MS media. Seedlings were incubated with 10µM PA (in DMSO) in the dark for 6 h at 21 °C. After 6 h, dexamethasone was added into the wells and returned to 21 °C for 36 h. Seedlings were then mounted in ½ MS for imaging.

2.8.2 Clearing/staining plants and checking for lignin inhibition

0.01% (w/v) Basic Fuchsin stain was prepared by first dissolving in ethanol (20% of final volume). Once dissolved, deionized water was used to bring the solution to the final volume. The solution of Basic Fuchsin was then filter sterilized with a 0.22µM filter. Arabidopsis seedlings treated with or without PA were cleared in methanol for 4 h at 25 °C followed by 10% (w/v) NaOH for 8 h at 60 °C. Cleared seedlings were stained with 0.01% Basic Fuchsin for 5 mins, transferred to 70% ethanol to destain for 10 mins, rehydrated with water and mounted in 50% glycerol (protocol from Dharmawardhana *et al.,* 1992). Stained seedlings were imaged using a Leica DMR epifluorescence microscope and excited at 560/40 nm, with emission collected at 595 nm.

2.8.3 Treating plants with 2,6-dichlorobenzonitrile

prLAC4:LAC4-mCHERRY and *prUBQ10:sec-mCHERRY* seeds were dark-grown for 3-5 days on GM agar (0.75%) plates and transferred to 24 well culture plates containing ½ MS. Seedlings were incubated with 10µM DCB (in DMSO) and 10 µM dexamethasone. Culture plates were returned to 21 °C for 36 h. Seedlings were then mounted in ½ MS for imaging.

2.9 Bright field light microscopy

Arabidopsis seedlings (3-5 day old) were imaged using a Leica DMR compound microscope equipped with 10x, 20x, 40x and 63x objective lenses. Samples were mounted in ½ MS (Murashige and Skoog) or 50% glycerol. Images were taken using the Qcapture digital camera (QImaging) and OpenLab imaging software as well as the Canon EOS Rebel T5 and EOS Utility software. Micrographs were processed using FIJI (Schindelin *et al.,* 2012).

2.10 Epifluorescence microscopy

Fluorescence screening and lignin autofluorescence of Arabidopsis seedlings (3-5 days old) were imaged using a Leica DMR compound microscope equipped with an EBQ 100 Isolated mercury lamp for excitation at 340-380 nm wavelength (ultraviolet). Filter cubes A (excitation filter same as bulb, emission filter at 400 nm), I3 (excitation filter at 450-490 nm, emission filter at 510 nm) and TX2 (excitation filter at 560/40 nm, emission filter at 595 nm). Samples were mounted in ½ MS (Murashige and Skoog) or 50% glycerol. Images were taken using the Qcapture digital camera (QImaging) and OpenLab imaging software as well as the Canon EOS Rebel T5 and EOS Utility software. Micrographs were processed using FIJI (Schindelin *et al.,* 2012).

2.11 Spinning disc confocal microscopy

The Perkin Elmer Ultraview VoX spinning disc confocal with Leica DMI6000 inverted microscope mount was used to image 3-5 day old seedlings. Samples were mounted in ½ MS and imaged using a 63x glycerol objective. Red fluorescent proteins were imaged using the 561 nm excitation laser and 595 nm emission filter. Acquisition settings for all lines were as follows: exposure = 500-1000ms and laser intensity = 15-30% Images were taken with a Hamamatsu 9100-02 CCD camera and the Volocity software. Micrographs were processed using FIJI (Schindelin *et al.,* 2012).

2.11.1 Using FRAP to measure protein mobility

FRAP measurements and analysis were done using the Volocity FRAP plugin. For all images, six pre-bleach images were obtained prior to bleaching (561 nm laser at 100%

intensity). Post-bleach images were taken at maximum speed either at 1) one image per sec for 60 or 120 secs or 2) one image per 20-30 secs for 300 secs. FRAP recovery curves were fitted using a single exponential equation ($f(t) = y + Ae^{-kt}$; t = time, y = mobile fraction, A = mobile fraction with bleach correction, k = the fluorescence at half time of recovery).

2.12 Mann-Whitney U test

Statistical comparisons for average mobile fractions and half time were done using the Mann-Whitney U non-parametric statistical test, run using the GraphPad™ Prism® software.

2.13 Arabidopsis T87 cell line culture

Arabidopsis thaliana T87 cells (ABRC) and T87 cells transformed with *VND7-GR* (Yamaguchi *et al.,* 2010) were kindly provided by our collaborators in Dr. Taku Demura's lab at the Nara Institute of Science and Technology (NAIST) in Japan. Cell cultures were sustained at 21 °C at 80-100rpm under 24 h light (fluorescence illumination at 75-125 µmol/m^2S) for seven-day cycles following subculturing to fresh Linsmaier and Skoog (LS) or GM liquid media with or without antibiotics (50µg/mL kanamycin). For experiments, cells containing the VND7-GR system (Kubo *et al.,* 2010) were cultured for 72 h under the same conditions before being treated with 10µM dexamethasone to induce protoxylem differentiation. After treatment, cells were returned to light at 21 °C at 80-100rpm for 24 h.

2.13.1 Isolating Arabidopsis cell microsomal and cell wall fractions

Arabidopsis cells were frozen in liquid nitrogen and ground to powder. The powdered cells (4 times volume in mL per 1 g weight of powdered cells) were transferred to pre-chilled

extraction buffer (50mM HEPES-KOH; pH7.5, 50% glycerol, 25mM KCl, 1x Roche protease inhibitor cocktail tablet) and stirred at 4 °C for 60 mins. After mixing, cells were pelleted for 10 mins at 38,00rpm. The cell wall containing pellet was preserved and resuspended with, solubilisation buffer (50mM HEPES-KOH; pH7.5, 25% glycerol, 25mM KCl, 2mM Na_2EDTA, 1%(w/v) Triton-X, 1mM DTT, 1x Roche protease inhibitor cocktail tablet) and kept stirring at 4 °C for 60 mins. The supernatant was transferred to a fresh tube and pelleted at 20, 000 rpm for 60 mins. Following centrifugation, the pelleted microsomal fraction was resuspended in solubilisation buffer and kept stirring at 4 °C for 60 mins. After the incubation, the microsomal fraction was pelleted for 5 mins at 4 °C at 5000 rpm. The supernatant was then transferred to a new tube to prepare for co-immunoprecipitation experiments.

2.13.2 Preparing crude cell lysate from Arabidopsis seedlings

Arabidopsis seedlings (*prLAC4:LAC4-Mcherry/VND7-GR, prUBQ10:LAC4-Mcherry/VND7-GR* and *prUBQ10:sec-mCHERRY/VND7-GR* plants) were treated with 10µM dexamethasone for 36 h at 21 °C. After incubation, seedlings were ground to powder in liquid nitrogen. After grinding, extraction buffer (50mM tris-HCl; pH7.5, 10mM $MgCl_2$, 500mM NaCl, 0.1% NP40, 1mM PMSF, 1x Roche protease inhibitor cocktail tablet) was added to the powder and vortexed quickly to suspend the ground plant matter. The mixture was then centrifuged at 15,000 x g for 25 mins at 4 °C. The pellet was discarded and the supernatant kept for further experiments.

2.14 Xylan Co-immunoprecipitation pull-down assay for Arabidopsis T87 cell lines

Dynabeads® (Life technologies™) were conjugated with xylan (LM10, CCRC-M138) and pectin (LM20) antibodies in accordance to the Dynabeads® protocol. Co-immunoprecipitation

experiments were conducted on both microsomal and cell wall fractions of Arabidopsis T87 cells (prepared as stated above) following the Novex™ Dynabeads® Co-Immunoprecipitation Kit protocol. Samples were tested for protein presence through SDS-PAGE and Western analysis with a Flamingo™ Fluorescent stain (Biorad™). Samples were subsequently sent for proteomic mass spectroscopy analysis at NAIST.

2.14.1 Laccase-RFP pull-down assays for Arabidopsis seedlings

Chromotek™ RFP-Trap® magnetic beads were prepared as specified by the RFP-TRAP® protocol. Pull-down assays were done on Arabidopsis seedlings (prepared as stated above) in accordance to the RFP-Trap® protocol. Protein presence was tested using SDS-PAGE and a Coomassie blue stain. Successful RFP pull-down was ascertained through Western analysis with an α-RFP (Invitrogen™) antibody.

2.14.2 Western blot

PVDF membrane with transferred proteins were blocked for 1 h at RT (or overnight at 4 °C) with 5% skim milk powder in TBST. After blocking, membranes were washed with TBST 3x (each for 5-10 mins at RT). Primary antibodies (α-RFP (Invitrogen™) or LM10 (PlantProbes)) in TBST was added and membranes were incubated for 1-2 h at RT (or overnight at 4 °C). Following 3x wash with TBST, membranes were incubated with secondary antibody (α-Rat) at RT for 1 h. Membranes were washed 3x in TBST and incubated for 1 min with Pierce™ ECL Western Blotting Substrate then imaged.

Chapter 3: Elucidating the Mechanism of Secondary Cell Wall Laccase Delivery

3.1 Introduction

The secretory pathway is a key player in the biosynthesis and modification of the plant cell wall. During 2CW synthesis, the cell has to make cell wall specific proteins and polysaccharides as well as deliver these 2CW components to the apoplast for cell wall formation. For proteins that are secreted to the 2CW, such as laccases, the secretory pathway begins with co-translational insertion into the endoplasmic reticulum (ER). Proteins targeted for secretion enter the ER lumen and are trafficked to the Golgi via COPII associated vesicles (reviewed by Kim and Brandizzi, 2015). Cell wall proteins are modified in the Golgi (as well as the ER) while cell wall polysaccharides (excluding cellulose and callose) are produced there. Cell wall proteins, such as laccases, are packaged at the TGN into secretory vesicles, which fuse with the plasma membrane, releasing the contents into the apoplast (Kim and Brandizzi, 2015).

The oxidative enzymes, LACCASE4 and LACCASE17, are required for the polymerization of monolignols into lignin in protoxylem tracheary elements, and these laccases localize in helical patterns in the 2CW (Schuetz *et al.,* 2014). While laccases' function and localization has been demonstrated, less is known about how laccases are packaged in vesicles and secreted to the apoplast, leading to the 2CW-specific localization. This question is part of a larger general question, which is how does vesicle trafficking change when cells shift from making 1CWs to 2CWs. The presence of 2CW in the helical pattern means a shift from a vesicle fusing with all parts of the plasma membrane in a diffuse trafficking pattern to vesicles fusing in the plasma membrane domains adjacent to the site of secondary cell wall synthesis, a domain of the

cortical cytoplasm rich in microtubules. These cortical microtubules have been shown to act as guides for proteins responsible for the recruitment of secretory vesicles to the proper 2CW location. Proteins VETH1/2 along with COG2 were shown to be important for tethering of the exocyst component EXO70A1 to the microtubule (Oda *et al.,* 2014) while EXO70A1 was shown to be responsible for recruiting post-Golgi vesicles carrying 2CW components to the microtubule (Li *et al.,* 2013).

The 2CW-specific location of laccases could be due to:

1) No change in vesicle trafficking pattern but a remobilization of laccases post-secretion to specific domains or,
2) A change in trafficking pattern redirecting vesicle flow to specific domains.

To test if vesicle traffic is rerouted to 2CW-specific domains during the shift from making 1CW to 2CWs, Arabidopsis seedlings in the VND7-GR inducible system were imaged before and after protoxylem TE differentiation.

Along with trafficking, the packaging of cell wall components into vesicles at the TGN is another area where much is still unknown. Knockout mutants of *ECHIDNA*, which encodes a TGN protein, showed mislocalization of proteins to multilamellar bodies while polysaccharides were mislocalized to the vacuole. The *echidna* mutant phenotype suggests that cell wall polysaccharides and proteins may be packaged in different vesicle populations at the TGN (McFarlane *et al.,* 2013). In contrast to this idea of separation of the cell wall polysaccharides and proteins in the secretory pathway, when developing protoxylem cells are treated with oryzalin (a microtubule depolymerizing drug), xylan and laccases mislocalized together in

aberrant secondary cell walls (Schuetz, unpublished). These experiments demonstrate not only that the microtubule cytoskeleton is required for the normal 2CW bands in their helical or spiral pattern, but it also suggests that laccase and xylan may be packaged and shipped in the same vesicle populations, with identical microtubule dependence.

Xylan (a major hemicellulose in 2CWs) is synthesized in the Golgi (Rennie and Scheller, 2004) while laccases are modified in the Golgi (Strong and Claus 2011). Studies in Arabidopsis on the 1CW arabinoxylan (a hemicellulose) was found to be covalently crosslinked with the protein arabinogalactan (Tan *et al.,* 2013), suggesting there may be other similar cases of crosslinking between proteins and polysaccharides. Since both are trafficked through the Golgi prior to being secreted to the 2CW, and both components are colocalized despite the loss of the 2CW helical bands in protoxylem TEs after oryzalin treatment, I hypothesized that the two components may be covalently crosslinked during 2CW formation.

The objective of this chapter was to test if laccase secretion to the 2CW of protoxylem tracheary elements occurs in a targeted manner, and if they are physically associated with xylan during 2CW formation.

3.2 Results

3.2.1 Laccases are secreted to secondary cell wall specific regions during protoxylem TE differentiation.

During protoxylem TE differentiation, when LAC4-mCherry was expressed using its native promoter (*proLAC4:LAC4-mCHERRY*), laccases were found only in the 2CW domains (Schuetz *et al.,* 2014). This localization pattern could be due to remobilization of laccases post-

secretion or a change in vesicle trafficking during protoxylem TE differentiation. To test these hypotheses, the localization of laccases was tracked in Arabidopsis seedlings containing the inducible VND7-GR system and transformed with a RFP-tagged laccase driven by a constitutive promoter (*proUBQ10:LAC4-mCHERRY*), which was active both before and during differentiation of the cells into protoxylem tracheary elements. Laccase localization was imaged in cells prior to protoxylem differentiation (figure 3.1A) and post-differentiation (figure 3.1B). Laccases localized to all regions of the 1CW of the cell in a uniform manner (figure 3.1A). In differentiated protoxylem cells, laccases were found to localize in bands which corresponded with the 2CW domains (figure 3.1B, white arrows). These domains were confirmed to be cellulose-rich 2CWs in previous studies using pontamine S4B stains (Schuetz *et al.,* 2014). In protoxylem TEs, laccase fluorescence was found to be greater in the 2CW than the 1CW, making laccases localized to the 1CW difficult to image by comparison (figure 3.1B). The change in localization suggests that secretory vesicle trafficking of laccases shifts from diffuse in 1CWs to directed to 2CWs domains during protoxylem TE differentiation.

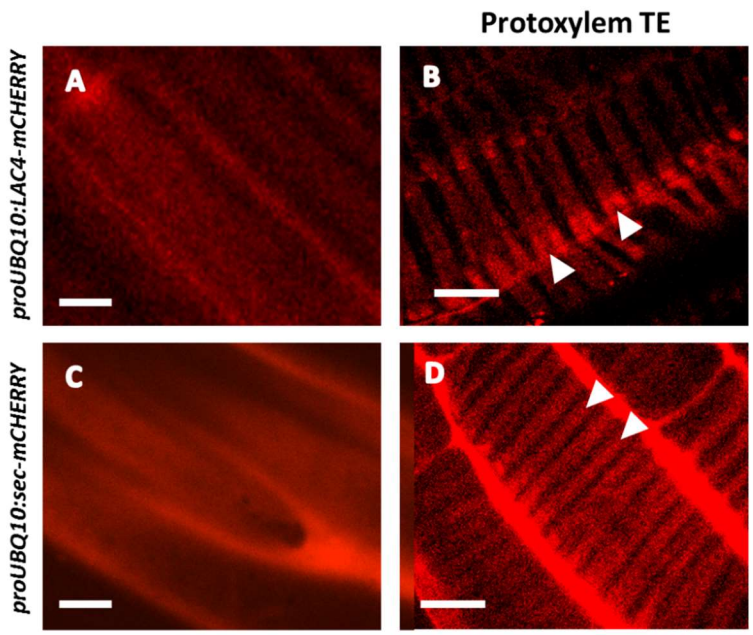

Figure 3.1: Laccases and small fluorescent proteins change from a uniform distribution to accumulating in the 2CW domains. Localization of LAC4 in Arabidopsis apical hook cells containing (A) the constitutive promoter-driven RFP-tagged LAC4 (*proUBQ10:LAC4-mCherry/VND7-GR*), or (B) the native promoter-driven RFP-tagged LAC4 (*proLAC4:LAC4-mCherry/VND7-GR)*. For comparison, (C and D) a secreted RFP (*proUBQ10:sec-mCherry/VND7-GR*) was expressed to demonstrate default protein traffic. Both secreted mCherry and RFP tagged laccase change from being found diffusely in the 1CW prior to xylem differentiation induction (A and C) to being distributed in 2CW specific domains (B and D) following induction. White arrowheads indicate 2CWs. Scale bar=5 µm.

3.2.2 Small fluorescent proteins are secreted to secondary cell wall specific regions during protoxylem TE differentiation

The secretion of a general protein (like a secreted fluorophore) could be different from the secretion of a cell wall specific protein (like laccases). Since laccase localization was found to shift from a diffuse pattern (pre-protoxylem TE differentiation at the 1CW) to a helical pattern (protoxylem TE cells at the 2CW), I wanted to test the hypothesis that a general secreted protein would have a similar shift in trafficking pattern pre/post-protoxylem differentiation.

To test this hypothesis, the localization of secreted RFP (*proUBQ10:sec*-mCHERRY) in Arabidopsis seedlings containing the VND7-GR construct was imaged prior to protoxylem TE

differentiation and post protoxylem TE differentiation (figure 3.1C and 3.1D). In cells with 1CW only, constitutively expressed secreted RFP was found to localize to all regions of the CW (figure 3.1C) much like constitutive laccase localization in 1CW (figure 3.1A). Post-protoxylem TE differentiation, secreted RFP localized to 2CW specific domains, much like with laccases (figure 3.1D and 3.1B). While secreted RFP localized to 2CW specific domains, unlike the laccases, these bands were less distinct (figure 3.1D). The similarity between laccase and secreted RFP localization pre/post-protoxylem TE differentiation suggests a change in vesicle flow from diffuse (during 1CW formation) to targeted (during 2CW) for secreted proteins in general.

3.2.3 Laccases and small fluorescent proteins are rapidly secreted and do not accumulate in the Golgi

2CW-related proteins moving between the Golgi and plasma membrane during protoxylem during formation of the spiral 2CW have been visualized previously, for example Golgi bodies containing CESA7 were tracked moving and pausing at 2CW bands (Watanabe *et al.,* 2015). To track the secretion of laccases and secreted RFP during trafficking to the 2CW, time course images were taken of Arabidopsis seedlings with the VND7-GR construct transformed with either 1) *proUBQ10:sec*-mCHERRY or 2) *proUBQ10:LAC4*-mCHERRY. Golgi containing laccases or secreted RFP were not observed (Figure 3.2; laccase data by Schuetz, unpublished, not shown). Secreted RFP can be seen accumulating in the 1CW from 12 to 24 h after protoxylem differentiation (figure 3.2) with visible 2CW beginning to form at 24 h (figure 3.2, white arrowheads). The lack of laccase and secreted RFP accumulating in the Golgi suggests the proteins may be secreted quickly or be below the limit of detection for the sensitivity of this spinning disk confocal.

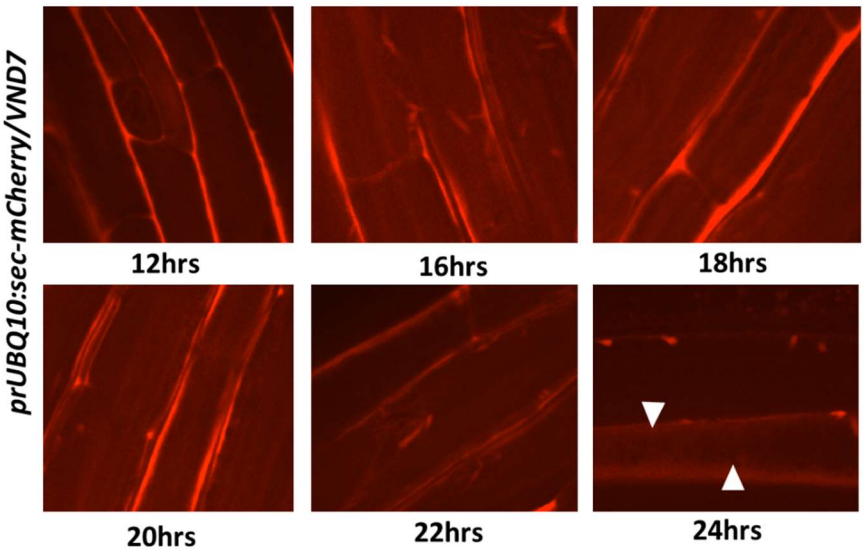

Figure 3.2: Small fluorescent proteins do not accumulate in the Golgi during secretion to the 2CW. Time course images taken of Arabidopsis *proUBQ10:sec-mCherry/VND7-GR* seedling hypocotyl cells at 12, 16, 18, 20, 22, and 24 h after induction to trigger protoxylem tracheary element differentiation. Secreted RFP (mCherry) is not seen accumulating in the Golgi during secretion to the cellular apoplast. White arrowheads point to the site of 2CWs beginning to form. Scale bar=5 µm.

To test if a secreted protein expressed at levels similar to CESA7 would be visible in the endomembrane system, a secreted yellow fluorescent protein driven by the *CESA7* promoter (*proCESA7:sec-mCITRINE*) was transformed into *proUBQ10:sec-mCherry* VND7-GR lines. The rationale for this experiment was that the constitutively expressed secreted RFP would label all of the primary cell wall domains prior to and during induction, but the *proCESA7:sec-mCITRINE* would be expressed only during secondary cell wall production, which would allow me to track the YFP appearance against an RFP background during xylem cell differentiation. Unfortunately, in these plants, the sec-mCITRINE was retained in an intracellular compartment that included nuclear envelope, ER-bodies, and cortical structures. Based on similarity of this pattern with the ER marker, GFP-HDEL, this compartment is the endoplasmic reticulum. Thus, it appears that the sec-mCIRTRINE was trapped in the ER, and it did not move further through the

endomembrane system (figure 3.3). Due to these technical problems, I was not able to track laccases as they moved through the endomembrane system.

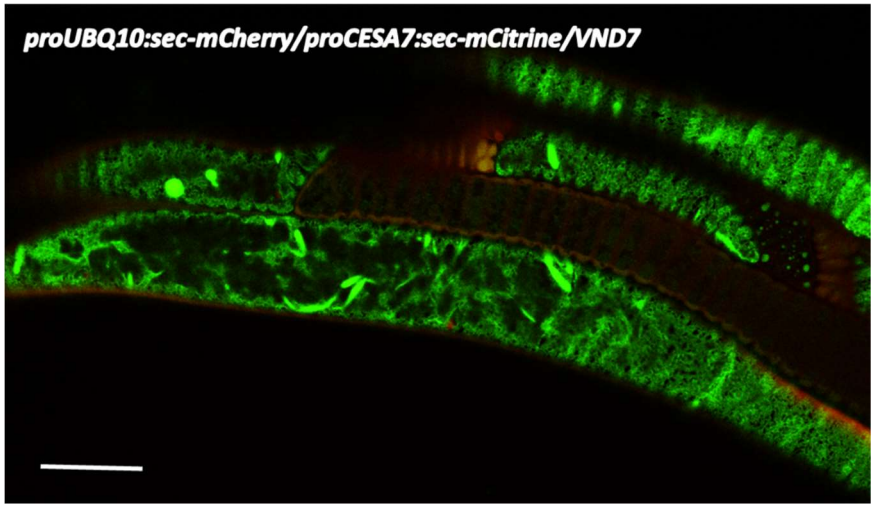

Figure 3.3: Secreted YFP is sequestered in the ER when driven by a CESA7 promoter. Arabidopsis seedlings transformed with *proUBQ10:sec-mCherry/proCESA7:sec-mCitrine/VND7* were imaged using the Perkin Elmer spinning disc confocal. Secreted RFP are found in all regions of the cell wall while the secreted YFP is seen retained in the ER. Scale bar=5 µm.

3.2.4 Xylan and laccases are not covalently cross-linked during secondary cell wall formation

To test if xylan and laccase are crosslinked during 2CW formation, co-immunoprecipitation (Co-IP) of Arabidopsis protoxylem TE cell culture lines induced by the VND7-GR protoxylem inducible system was done. Magnetic beads were conjugated with anti-xylan antibodies CCRC-M138 and LM10. Co-IP pulldown was performed on both microsomal and cell wall fractions. To test if pulldown assays were successful, Western blots were conducted and protein presence was identified using the Flamingo© protein stain. The initial background protein level was determined in pull-downs down with unconjugated beads (figure 3.4A). Enrichment of proteins in lanes pulled-down by the first anti-xylan antibody CCRC-M138 were present in the microsomal fraction gel (figure 3.4B) and in the cell wall fraction (figure 3.4C). For the second anti-xylan antibody, LM10, enrichment was present in the microsomal fraction but not in the cell wall fraction (figure 3.4B and 3.4C). Since enrichment could be seen

in the microsomal fraction and cell wall fractions, samples were analyzed using mass spectrometry (table 3.2, done in the Demura lab, at the Nara Institute of Science and Technology, NAIST, Japan). Neither laccases, nor any other cell wall-related proteins, were found on the list of proteins pull-down with anti-xylan antibodies, suggesting xylans are not strongly cross-linked with laccases (or any other cell wall proteins) during secretion to/at the cell wall (table 3.2).

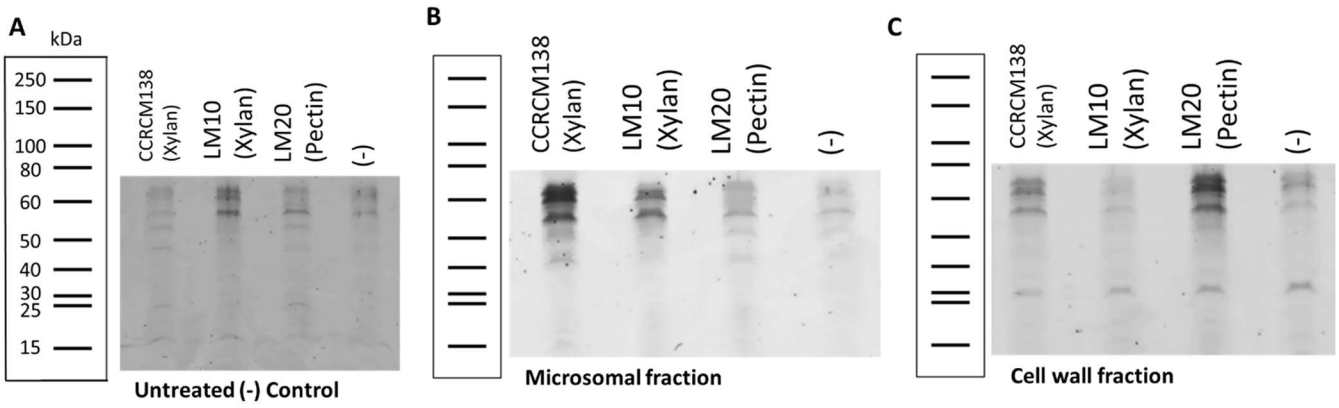

Figure 3.4: Enrichment of proteins (stained by Flamingo protein stain) pulled down by CCRC-M138 anti-xylan antibody in microsomal and cell wall fractions. Representative (n=3) Western blots shown. Western blots were used to identify successful Co-IP pulldown experiments. Flamingo protein stains were used to determine the presence of overall proteins in the Co-IP pulldown experiments in (A) unconjugated bead pulldown, (B) microsomal fraction pulldown, and (C) cell wall fraction pulldown. Band enrichment is visible for both CCRC-M138 lanes (B and C) when compared to (A), suggesting successful pulldown of xylan using CCRC-M138. Band enrichment is visible for LM10 was only visible for the microsomal fraction pulldown (B) when compared to (A), suggesting successful pulldown of xylan in microsomal fraction with LM10 but not in the cell wall fraction. Ladder = New England Biolabs® nonstained ladder (P77035).

Table 3.2: Mass spectrometry analysis of xylan pulldown shows no cell wall related proteins associating with xylan. Mass spectrometry analysis of Co-IP pulldown assays on microsomal fractions for α-xylan antibodies CCRC-M138 and LM10, α-pectin antibody LM20 and non-conjugated bead controls. No cell wall related proteins were identified in the pulldown experiment.

Antibody	TAIR ID	Name
M138	AT3G50920.1	Phosphatidic acid phosphatase (PAP2) family protein
	AT5G10160.1	Thioesterase superfamily protein
	AT1G11360.1	Adenine nucleotide alpha hydrolases-like superfamily protein
	AT1G55970.1	HAC04, HAG04, HAC4, HAG4, HAC6 | histone acetyltransferase of the CBP family 4
	AT5G64440.1	AtFAAH, FAAH | fatty acid amide hydrolase
	AT5G06900.1	CYP93D1 | cytochrome P450, family 93, subfamily D, polypeptide 1
LM10	AT3G50920.1	Phosphatidic acid phosphatase (PAP2) family protein
LM20	AT3G50920.1	Phosphatidic acid phosphatase (PAP2) family protein
	AT4G08690.1	Sec14p-like phosphatidylinositol transfer family protein
	AT1G74540.1	CYP98A8 | cytochrome P450, family 98, subfamily A, polypeptide 8 |
	AT5G08750.1	RING/FYVE/PHD zinc finger superfamily protein
(-)	AT3G50920.1	Phosphatidic acid phosphatase (PAP2) family protein
	AT5G10170.1	ATMIPS3, MIPS3 | myo-inositol-1-phosphate synthase 3
	AT1G20670.1	DNA-binding bromodomain-containing protein

Since Co-IP is a technique developed and optimized for protein systems, the converse experiment of pulling down xylan with RFP-tagged laccases was also tested. Arabidopsis seedlings (VND7-GR background), transformed with either 1) *proUBQ10:sec*-mCHERRY, 2) *proUBQ10:LAC4*-mCHERRY or 3) *proLAC4:LAC4*-mCHERRY) were induced to form ectopic protoxylem TE. RFP-TRAP© magnetic beads, able to bind the mCherry RFP fluorophore, were used due to a strong laccase antibody not being readily available. Western blot analysis (using an anti-RFP) on pull-downs were done to check for enrichment of bands at ~28KDa (size of RFP) and ~90KDa (size of laccase tagged with RFP). Bands at ~28KDa are enriched for pulldowns done on Arabidopsis seedlings containing the *proUBQ10:sec-mCHERRY* construct (figure 3.5A).

Enrichment of ~90KDa bands are also visible for both *proUBQ10:LAC4-mCHERRY* and *proLAC4:LAC4-mCHERRY* lanes (figure 3.5B and 3.5C), indicating that both free RFP in the control and RFP-tagged LAC4 had been captured by the anti-RFP-beads. To test if these proteins were associated with xylan, Western blot analysis using an anti-xylan antibody (LM10) was done on the *LAC4-mCHERRY* or *sec-mCHERRY* control pulldowns. Coomassie blue stain was first done to detect the presence of overall protein (figure 3.6A) followed by Western analysis (figure 3.6B). No bands are present in any of the three different Arabidopsis lines at the ~90KDa size (figure 3.6B, black arrow). This suggests that unlike the 1CW arabinoxylan and arabinogalactan (Tan *et al.,* 2013), 2CW laccases and xylan are not crosslinked during secretion to the 2CW.

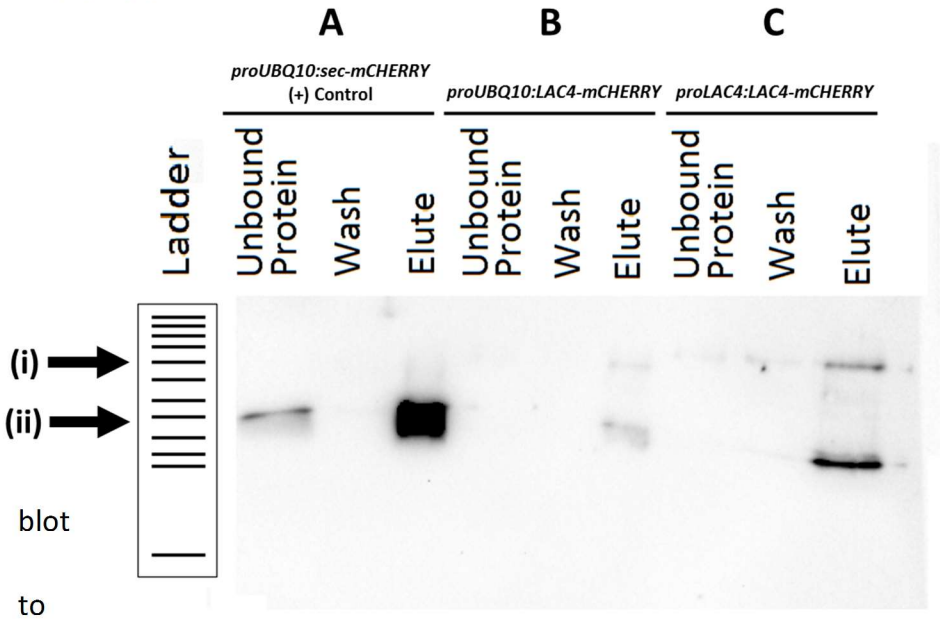

Figure 3.5: RFP tagged laccase (LAC4-mCherry) and secreted RFP (mCherry) labelled with anti-mCherry following RFP-TRAP© pulldown. Western blot using α-mCherry antibodies was done to determine if pulldown assays using Chromotek RFP-TRAP© magnetics beads were successful. Enrichment (comparing unbound protein to elute lanes) is visible for all three pulldown experiments (A) secreted mCherry, (B) mCherry-tagged laccase driven by a ubiquitous promoter and (C) mCherry-tagged laccase driven by a native promoter, at the expected protein sizes (i) mCherry = 28KDa (A), and (ii) laccase-mCherry = 90KDa (B-C). Ladder = BLUelf prestained protein ladder from GeneDirex®.

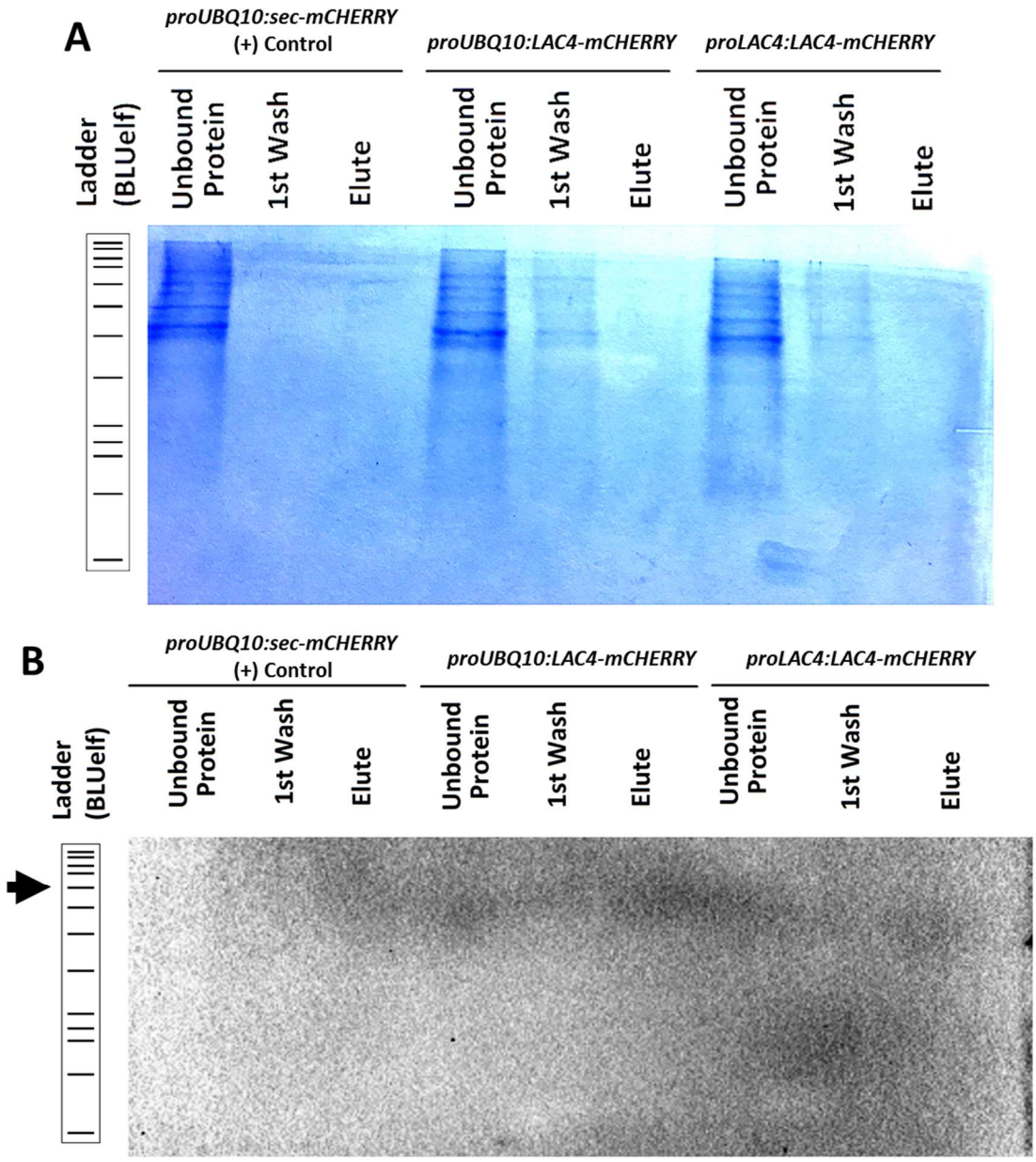

Figure 3.6: Western blot analysis shows no evidence of xylan and laccase covalent crosslinking. Western blot analysis using an α-xylan antibody (LM10) detected no xylan pulled-down with Chromotek RFP-TRAP© magnetics beads (B). Staining with coomassie blue shows proteins present in all lanes (A) but no bands are detectable at the expected band size (B, ~90KDa, black arrow) indicating no cross-linkage between xylan and laccase. Ladder = BLUelf prestained protein ladder from GeneDirex®.

3.4 Discussion

LAC4 and LAC17, two laccases required for the lignification of 2CWs, were previously shown to localize to 2CW specific domains (Schuetz *et al.*, 2014). These laccases were found localized to only 2CW domains and not within the 1CW domains of protoxylem TEs, suggesting either a post-Golgi secretory vesicle trafficking pattern change or a reorientation of proteins post-secretion. Here, in differentiating protoxylem TEs, fluorescence localization of both an RFP tagged laccase and a generic secreted RFP suggests a model of vesicles shifting from a nonpolar to a polar trafficking pattern. The use of a ubiquitin promoter allowed me to contrast laccase localization prior to protoxylem TE differentiation, where ectopically expressed laccases were found secreted to all regions of the 1CW, with the native 2CW pattern. The lack of the helical banding pattern seen in the 1CW suggests laccases follow the default secretory pathway prior to xylem differentiation before shifting to a targeted vesicle secretory pattern during TE differentiation.

To ascertain if only laccase-containing vesicles are shifting during protoxylem differentiation, or if there is a general shift in secretion, a generic secreted fluorescent protein (sec-RFP) was also studied. Prior to protoxylem TE differentiation, sec-RFP was localized to all regions of the cell, similar to laccases. Post-differentiation, the secreted fluorophore localized to 2CW specific domains, which is reminiscent of the deposition pattern of laccases. This suggests vesicle trafficking is generally shifted from diffuse to targeted during the change of secretory demand occurring during the formation of 2CWs in protoxylem TE. While the deposition patterns between LAC4 and secRFP are similar, it should be noted the fluorescence signal in the apoplast was brighter and less distinct in the secreted fluorophore micrographs

than in laccase localization micrographs. This could be due to more accumulation of the secreted fluorophore, which is smaller in size (28KDa) than LAC4 (62KDa).

The above data suggest that vesicle trafficking shifts from diffuse to targeted, revealing a possible mechanism where cellular vesicle trafficking is reoriented during 2CW formation. Many examples of vesicle traffic shifting from diffuse to targeted can be found in plants. One example of vesicle traffic shifting during different life stages of the cell is found in the symbiosis between cortical root cells and arbuscular mycorrhizal fungi. Prior to fungus symbiosis, the *Medicago* phosphate transporter MtPT4 is found secreted to all regions of the plasma membrane. This nonpolar secretion is changed upon fungus-root cell symbiosis, where MtPT4 secretion becomes targeted only to regions shared between the cortical root cell and the invading fungus (Pumplin *et al*., 2010). PIN proteins, auxin transporters, undergo a similar shift in trafficking pattern from diffuse to targeted (Feraru and Friml, 2008). This redirection of PIN proteins is achieved through the regulation of PIN recycling. PIN proteins are first synthesized and secreted to all regions of the plasma membrane in a nonpolar manner. Upon phosphorylation by members of the AGC family, PIN proteins are recycled and their apical/basal polarity is established (Feraru and Friml, 2008). Although laccases follow a similar pattern of being diffuse in the 1CW, laccases do not have predicted phosphorylation sites (http://phosphat.uni-hohenheim.de/) nor is there evidence they are recycled, making it unlikely that PIN and laccase share a similar mechanism of polarized secretion.

The formation of the cell plate during cytokinesis is another example of polarized secretion in plants. During the start of cytokinesis, vesicle trafficking becomes targeted to the division zone of the dividing cell to form the cell plate. These vesicles have been shown to be

closely associated with the microtubules of the phragmoplast (reviewed by Van Damme *et al*., 2008). KNOLLE, a cytokinesis-specific syntaxin, localizes to the division zone during the formation of the cell plate and is involved in mediating its formation (Lukowitz *et al*., 1996; Lauber *et al*., 1997). When expressed in non-proliferating cells, KNOLLE proteins localized diffusely to the plasma membrane in tip-growing root hairs, suggesting KNOLLE protein-containing vesicles may be misdirected due to a loss of sorting signals usually present during cytokinesis or a general redirection of vesicle flow during cytokinesis (Völker *et al*., 2001). The pattern of KNOLLE secretion in non-proliferating cells vs proliferating cells is reminiscent of the secretory pattern of laccases in non-differentiating cells and differentiating protoxylem cells, suggesting similar mechanisms of polarized secreted may be utilized.

Polarized secretion in protoxylem tracheary elements has been proposed to be mediated by the exocyst complex, as loss of one part of the complex, EXO70A1, has been demonstrated to caused the formation of abhorrent 2CW patterns (Li *et al.,* 2013). The exocyst complex is a conserved complex of proteins involved in assisting the tethering of vesicles to the plasma membrane during vesicle fusion. In mammalian and yeast cells, the exocyst complex is made up of 8 proteins (Sec3, Sec5, Sec6, Sec8, Sec10, Sec15, Exo70 and Exo84) and while homologues are present in plants, whether they form a similar complex is not yet determined. Plants have expanded exocyst gene families, for example, the *EXO70* gene family in Arabidopsis has 23 homologues. (Synek *et al*., 2006). In developing protoxylem cells, EXO70A1 is associated with cortical microtubules through the vesicle tethering proteins 1/2 (VETH1 and 2) and Golgi complex 2 protein (COG2) complex, suggesting EXO70A1 is an important exocyst protein involved in the secretion of 2CW cargo (Oda *et al.,* 2014). Since EXO70A1 has been

demonstrated to be involved in the trafficking of 2CW components, laccase containing vesicles could be tethered to the plasma membrane via this EXO70A1-containing exocyst complex.

Since secreted 2CW components traverse the Golgi prior to secretion to the plasma membrane, I predicted that one way to track the trafficking of laccase during protoxylem differentiation would be to track the Golgi bodies moving in the cytosol of the cell. Previous studies by Watanabe *et al.* (2015) tracked the movement of the CESA7 in the Golgi, and found CESA7-containing Golgi bodies paused at 2CW bands during 2CW formation. To gain further insight on the shift of secretory vesicle trafficking, time course experiments were done to track movement of laccases and secreted RFP over the stages of cellular differentiation. Though laccases and secreted RFP could be seen in the cell wall, laccase and secreted RFP intracellular signals were almost always undetectable (with laccases accumulating in a few Golgi on very rare occasions). This data suggests that laccase and secreted RFPs are secreted quickly, or laccases are secreted via a non-canonical secretion independent of the Golgi apparatus. Laccases contain both predicted N-terminal signal peptide sequences as well as N and O glycosylation sites (Turlapati *et al.,* 2011), suggesting they are secreted via the endomembrane system. One experiment that could confirm whether laccases are secreted via the endomembrane system or not is through the use of the secretory pathway and subcellular traffic inhibitor Brefeldin A (BFA). BFA is a drug known to disrupt post-Golgi secretion and sequester proteins into compartments that are composed of trans-Golgi network and endosomes (reviewed by Nebenführ *et al*., 2002). These compartments have been termed “BFA compartments” (reviewed by Nebenführ *et al*., 2002). If laccases accumulate in BFA compartments in *proLAC4:LAC4-mCHERRY* transformed plants treated with BFA, then this is

evidence that, as predicted by their signal sequence and glycosylation sites, laccases are secreted to the cell wall via the endomembrane system. Thus, the difficulty in detection of tagged LAC4 within the Golgi would likely be due to laccases being secreted quickly and only within the Golgi apparatus transiently.

While laccases and secreted RFPs were not expressed at levels that could be visualized during secretion, another 2CW protein, CESA7, has been successfully tagged and found to accumulate in the Golgi, making visualization of CESAs during xylem development possible (Watanabe *et al*., 2015). Though attempts were made to track the vesicle traffic of secreted YFP (driven by a CESA7 promoter) against the RFP already in cell wall, secreted YFP proteins became sequestered in the ER. Though no ER retention sequence (such as HDEL) was found within the sequence, the YFP did not progress through the endomembrane system. One possibility for the YFP being retained in the ER could be an unintentional introduction of stress on the cell system due to the introduction of too many foreign, highly expressed secreted proteins.

An important element of targeted secretion of LAC4 to secondary cell wall thickenings could be the proper assembly of secretory vesicles with appropriate SNARES, Rabs, or exocyst proteins on their surface (Uemura, 2016). The importance of proper assembly of secretory vesicles was highlighted by analyses of mutants of the TGN protein, echidna (Gendre/McFarlane *et al.*, 2013; Gendre *et al*., 2011). The *echidna* mutant phenotype was mislocalization of cell wall polysaccharides to vacuoles and membrane proteins to multilamellar bodies, suggesting polysaccharides and membrane proteins may utilize different mechanisms during packaging at the trans-Golgi network (McFarlane *et al*., 2013). In contrast, while treatment with the microtubule depolymerization drug (oryzalin) causes the loss of 2CW bands,

xylan and laccase remain localized together suggesting proteins and polysaccharides are trafficked together to the cell wall (Schuetz, unpublished).

Cell wall polysaccharides like pectin and xylan are synthesized in the Golgi before being secreted to the cell wall (Rennie and Scheller, 2014) while 2CW proteins such as the heavily glycosylated laccases also traverse the Golgi and are modified there (Strong and Claus, 2011). Crosslinkage between 1CW arabinoxylan and the arabinogalactan protein were also demonstrated by Tan *et al.* (2013) suggesting there may be other cases of protein and polysaccharides being covalently bound. Co-IP done to ascertain covalent bonding between xylan and laccase in soluble, microsomal and cell wall fractions revealed the failed to produce evidence the are crosslinked during secretion nor at the cell wall.

Analysis of proteins pulled down by Co-IP experiments reveals a wide range of proteins unrelated to the cell wall. One explanation for the wide variety of proteins seen in the pulldown could be the nature of the cell wall. Xylan is a hemicellulose with many side chains, making the polysaccharide sticky and able to potentially pull down proteins from the cytoplasm during sample preparation. Another possible cause for the variety of non-cell wall proteins detected is that Co-IP is a technique that is widely used for studying protein-protein interactions, rather than protein-polysaccharide interactions. It is not optimized to detect specific interactions between xylan and cell wall proteins, but this may be possible by optimizing the experimental process.

In this chapter, I examined how RFP laccase or a secreted RFP are localized during either 1CW formation or during protoxylem TE 2CW formation, and it was clear that during 2CW

formation there was a general shift in secretory activity. I speculate that the exocyst complex and associated microtubule tethering proteins play an important role in the shift in vesicle trafficking during 2CW secretion to the PM. This apparently broad change in the secretory pathway may indicate that 2CW components are moving in shared vesicle populations, but pull-down assays show that xylan and laccases are not crosslinked during post-Golgi secretion. This may provide insight into the nature of polysaccharide and protein packaging during 2CW secretion, and is consistent with the mutant studies on *echidna* that suggest there are different populations of post-TGN secretory vesicles. However, I cannot exclude the possibility that these components are packaged together in vesicles, without covalent linkage. Overall, my study supports a protoxylem TE differentiation model where laccases are able to direct lignification due to their 2CW localization, which is the result of the general reorientation of secretory vesicle flow of not only laccases but other cell wall proteins to the microtubule and exocyst-rich plasma membrane adjacent to the growing 2CW.

Chapter 4 : Laccase Localization is Due to Immobility in the Secondary Cell Wall

4.1 Introduction

The current view of lignification is that monolignols are diffusely secreted by lignifying cells and their neighbours, then the pattern of lignification is established by the presence of oxidizing enzymes in the cell wall, such as peroxidases (Lee, *et al.,* 2013) and/or laccases (Schuetz *et al.,* 2014). Schuetz *et al.* (2014) demonstrated through localization studies that laccases localize to 2CW domains in protoxylem TEs but are absent in the 1CWs. Although laccase double/triple mutant studies have been used to show that laccases are important for the lignification of 2CW in xylem cells (Zhao *et al.,* 2013; Berthet *et al.,* 2011), it is unknown what constrains laccases to these 2CW domain.

Protoxylem TE 2CWs are deposited in annular or helical patterns and contain both primary and secondary cell wall domains (Turner *et al.,* 2007). The two cell walls differ in their composition, microfibril organization, mechanical properties and matrix polymer structure/mobility (Cosgrove and Jarvis, 2012). Laccases could be found specifically in 2CW domains due to two mechanisms:

1) Laccase exclusion from the 1CW, perhaps due to the gel-like matrix of the 1CW pectin, or
2) Laccase confinement to the 2CW due to binding by the 2CW components.

To test these two possibilities, I used fluorescence recovery after photobleaching (FRAP), a powerful tool that is used to determine the movement/mobility of proteins, which has been used in a number of cell wall studies. Martinière *et al.* (2012) used FRAP to study the movement of plasma membrane proteins and found the cell wall was a major factor in

constraint of plasma membrane proteins' lateral diffusion. In addition, Watanabe *et al.* (2015) used FRAP to study the delivery of cellulose synthase complexes (CSCs) to the plasma membrane during cellulose synthesis. To test whether the restriction of laccase to the 2CW domains is due to 1CW exclusion or 2CW constraint, FRAP experiments were conducted on Arabidopsis seedlings in the VND7-GR background. The mobility of both a secreted RFP and RFP tagged laccase were tracked by recording the speed and intensity of FRAP in either 1CW or 2CW regions.

4.2 Results

4.2.1 Characterization of a control fluorescent protein mobility in both the primary and secondary cell walls.

The primary and secondary cell wall environments are different given their different composition and organization (Cosgrove and Jarvis, 2012). To test if there is a difference in the mobility of a control protein in these two cell wall environments, a secreted fluorescent protein (sec-mCherry) was engineered using the N-terminal signal sequence from a lipid transfer protein gene, driven by the *Ubiquitin10* constitutive promoter (Schuetz, unpublished), as proteins targeted to the endoplasmic reticulum by the signal sequence are predicted to follow a default secretion pathway to the cell wall (Alberts *et al.,* 2015).

FRAP experiments were conducted on the mCherry in both the primary and secondary cell wall (figure 4.1A-D). FRAP experiments are able to explore the mobility of proteins tagged with fluorophores in a specified region of interest (ROI). The fluorescence of the tagged proteins in the ROI are permanently photobleached, allowing the measurement of the mobility

of neighbouring tagged proteins. After measuring the mobility of neighbouring proteins (with fluorophore tags), recovery curves were extracted from the normalized fluorescence intensity data. The fraction of recovered fluorescence over the initial fluorescence (mobile fraction, F_m) as well as the half time (in seconds) of overall fluorescence recovery (T½) was calculated. The F_m is the fraction of fluorescence recovered, which can be converted to a percent through F_m*100%, and an indicator of protein mobility. The T½ is a measure of the speed with which the recovered fluorophore tagged proteins move. Mobile proteins tend to have F_m greater than 0.5 while immobile proteins tend to have F_m less than 0.5 while a lower T½ indicates a fast moving protein and a higher T½ indicates a slow moving protein.

Plants containing both a secreted fluorophore (*proUBQ10:sec-mCHERRY*) and the inducible *VND7-GR* construct were measured in 1CW (before) and in 2CW after protoxylem TE differentiation. In undifferentiated cells, which contain only a 1CW, fluorescence was recovered after photobleaching in the region of interest (ROI) in quick succession through lateral diffusion (figure 4.1A). Fluorescence recovery curves show 72% fluorescence recovery for secreted RFP in the 1CW (figure 4.1C). In contrast, in the 2CW region of protoxylem TE cells, the fluorescence was not recovered in the bleached region (figure 4.1B) with 22% fluorescence recovery for secreted RFP in the 2CW (figure 4.1D). The averaged calculated half time of recovery (T½) was also longer for secreted RFP in the 2CW (T½ = 4.4 ± 7.5) than in the 1CW (T½ = 2.3 ± 1.0). These fluorescence recovery patterns demonstrate that secreted RFP may be more mobile in 1CW than in the 2CW environment (figure 4.1E), suggesting the difference in cell wall composition or organization can play an important role in protein mobility in the two cell wall environments.

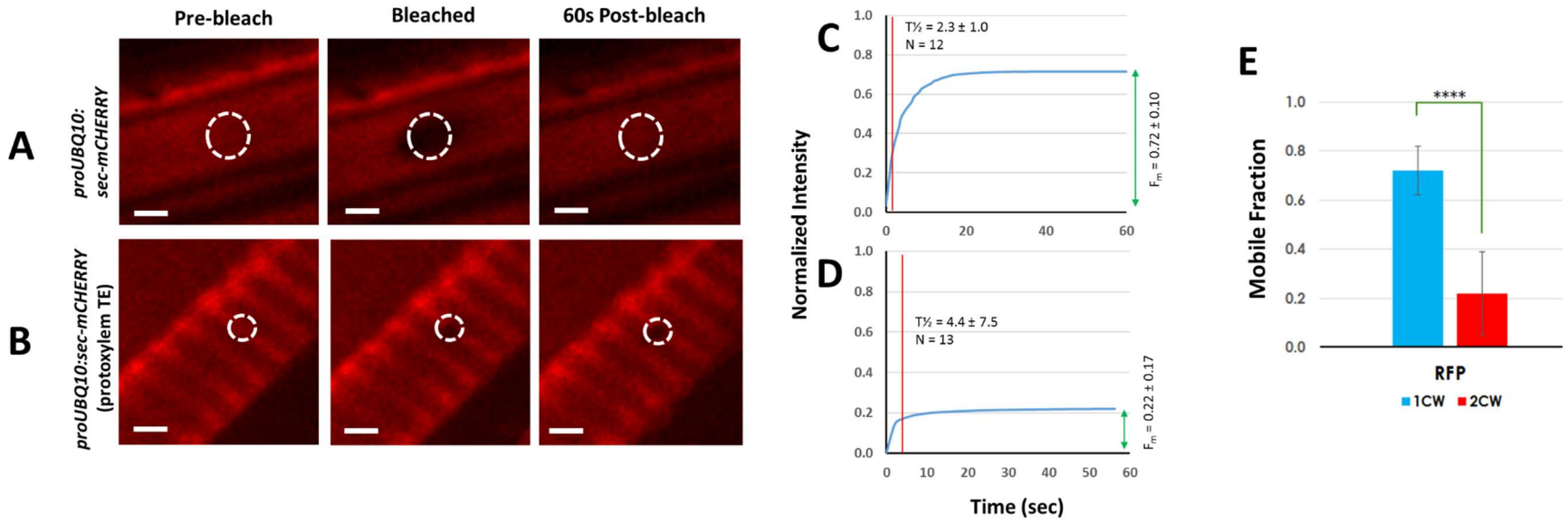

Figure 4.1: Secreted RFP (mCherry) is mobile in the 1CW and immobile in the 2CW. FRAP images taken of Arabidopsis seedling apical hook cells containing *proUBQ10:sec-mCherry/VND7-GR* before bleaching the region of interest (ROI, white dashed circles), at the time of bleaching the ROI and 60 secs after bleaching the ROI. (A) Prior to differentiation to protoxylem TEs, secreted mCherry rapid fluorescence recovery over the course of the 60 sec FRAP experiment. (B) 36 h after protoxylem TE differentiation, secreted mCherry very slow fluorescence over the course of the 60 sec FRAP experiment. Measurements were taken every 1 sec over a 60 sec period. The mobile fraction (Fm, green double arrows) and T½ (represented by a red line on the curves) were calculated for FRAP experiments done on (C) cells prior to protoxylem differentiation and (D) cells 36 h after protoxylem differentiation. (E) The mobility (F_m) of the secreted mCherry in the 2CW was found to statistically decrease (Mann Whitney U test, $P \leq 0.0001$) when compared to the mobility of secreted mCherry in the 1CW. Scale bar = 3 µm. Error bars = SD.

4.2.2 Using FRAP to elucidate the mobility and speed of laccases in both the primary and secondary cell wall

As detailed in the introduction chapter of this thesis, laccases are oxidative enzymes that facilitate the polymerization of monolignols to lignin, an important component of the 2CW (Strong and Claus, 2011). These oxidative enzymes have been localized to 2CW domains (Schuetz *et al.,* 2014), but it unknown why they are found in 2CW-specific domains and not in the 1CW. In this study, the mobility of a laccase, *LACCASE4 (LAC4)* was examined, as LAC4 is one of three laccases that has been demonstrated to be important for lignification in Arabidopsis stems (Zhao *et al.,* 2013).

To test if LAC4 mobility is similar to the secreted RFP mobility described above, FRAP experiments were conducted to measure the mobility of the LAC4 in both primary and secondary cell walls (figure 4.2A-E). Laccases were fused to an RFP (mCherry) fluorescent protein and either expressed ectopically in 1CW using a constitutive promoter (*proUBQ10:LAC4-mCHERRY*) (figure 4.2A) or expressed in the 2CW using the native promoter (*proLAC4:LAC4-mCHERRY*) (figure 4.2B). All experiments were done in the *VND7-GR* background. Ectopically expressed LAC4-mCherry in the 1CW had a similar mobility pattern as secreted RFP, with the fluorescence recovering quickly post-bleach through lateral diffusion (figure 4.1A and 4.2A). The very slow mobility of RFP tagged LAC4 in the 2CWs of protoxylem TEs was also comparable to the secreted RFP (figure 4.1B and 4.2B). The recovery was so slow that the ROI appeared permanently bleached, and it did not recover mobility even after allowing for recovery for 60 secs (figure 4.2B). To test if the fluorescence would recover given a

longer time period, fluorescence recovery was monitored over 5 mins, yet very little recovery was detected (figure 4.3).

A larger mobile fraction of fluorescently tagged LAC4-mCherry migrated into the ROI in the 1CW (figure 4.2C, $F_m = 0.72 \pm 0.10$) than LAC4-mCherry in the 2CW (figure 4.2D and 4.2E, $F_m = 0.22 \pm 0.17$). The averaged calculated T½ of RFP tagged laccase in the 1CW (figure 4.2C, T½ = 8.1 ± 2.2) was faster than the averaged calculated T½ of RFP tagged laccase in the 2CW (figure 4.2D, T½ = 20.7 ± 25.0). Together, this suggests that laccases have a similar mobility pattern as secreted RFP in both the 1CW and 2CW. Quantification of multiple FRAP experiments demonstrated that laccases are significantly more mobile in the 1CW than in the 2CW (figure 4.2E). Therefore, the hypothesis that the pectin-rich primary cell wall is excluding LAC4 from the 1CW is less likely, but rather it appears that LAC4 is bound to the 2CW. Candidates for components that bind laccases to the 2CW are the major 2CW hemicellulose, xylan, the biopolymer lignin, or the more abundant/ordered 2CW cellulose.

Despite both RFP-tagged LAC4 and secreted RFP having a similar pattern of mobility in the two different cell wall environments (1CW versus 2CW), laccases were found to be less mobile than secreted RFP in the 2CW when compared using the Mann Whitney U statistical tests (figure 4.4A and 4.4B). While a similar percent of fluorescence was recovered in the photobleached ROI of laccases and secreted RFP in the 1CW, in the 2CW, which is the environment in which laccases are typically found, the mobile fraction of RFP tagged laccases was lower and its half-time of recovery longer than secreted RFP fluorescence (figure 4.4A). The T½ of laccases in both the 1CW and 2CW were longer than secreted RFP, suggesting slower mobility during recovery (figure 4.4B).

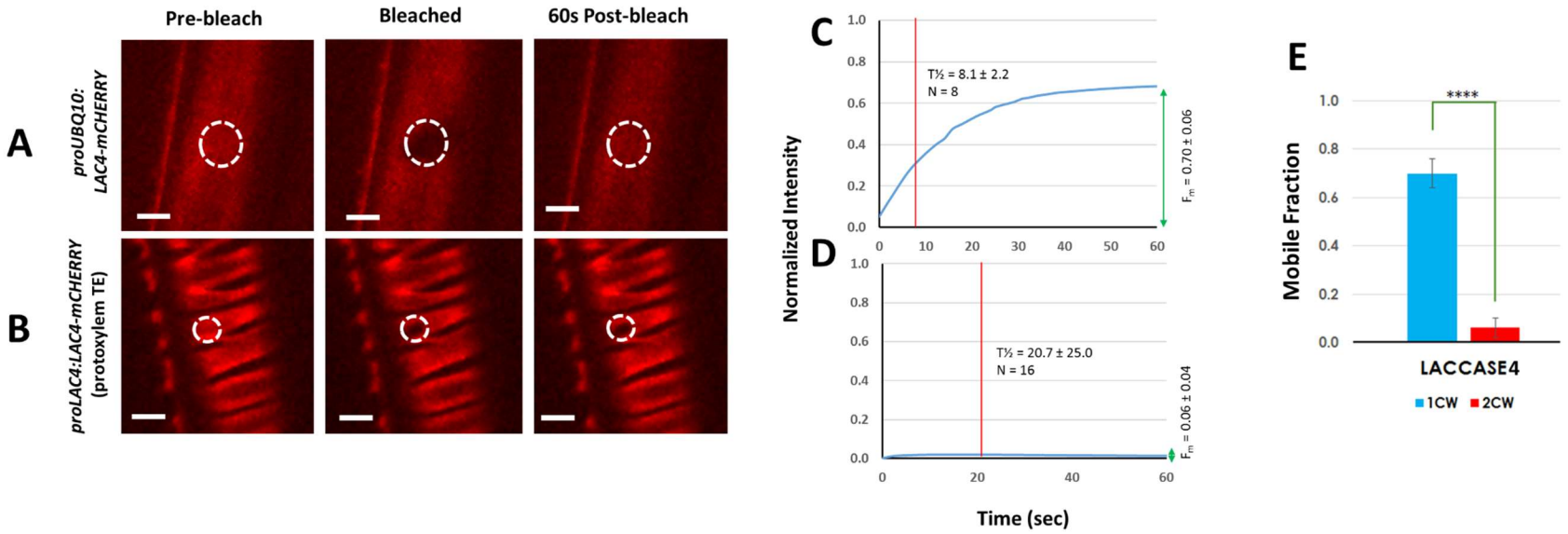

Figure 4.2: Laccases are mobile in the 1CW and immobile in the 2CW. FRAP images taken of Arabidopsis seedling apical hook cells containing (A) *proUBQ10:LAC4-mCherry/VND7-GR* or (B) *proLAC4:LAC4-mCherry/VND7-GR* before bleaching the ROI (white dashed circles), at the time of bleaching the ROI and 60 secs after bleaching the ROI. (A) Prior to differentiation to protoxylem TEs, RFP tagged laccase fluorescence recovers rapidly over the course of the 60 sec FRAP experiment. (B) 36 h after protoxylem TE differentiation, RFP tagged laccase fluorescence in the 2CW does not recover over the course of the 60 sec FRAP experiment, Measurements were taken every 1 sec over a 60 sec period. The mobile fraction (Fm, green double arrows) and T½ (represented by a red line on the curves) were calculated for FRAP experiments done on (C) cells prior to protoxylem differentiation and (D) cells 36 h after protoxylem differentiation. (E) The mobility (F_m) of the RFP tagged laccase in the 2CW was found to statistically decrease (Mann Whitney U test, $P \leq 0.0001$) when compared to the mobility of RFP tagged laccase in the 1CW. Scale bar = 3 µm. Error bars = SD.

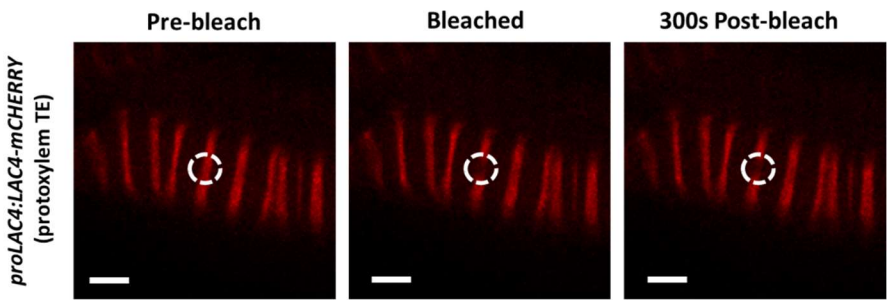

Figure 4.3: Laccases are immobile in the 2CW of protoxylem TEs FRAP images taken of Arabidopsis seedling apical hook cells containing *proLAC4:LAC4-mCherry/VND7-GR* before bleaching the ROI (white dashed circles), at the time of bleaching the ROI and 300 secs after bleaching the ROI. 36 h after protoxylem TE differentiation, RFP tagged laccase fluorescence does not recover over the course of the 300 sec FRAP experiment suggesting it is immobile in the 2CW.

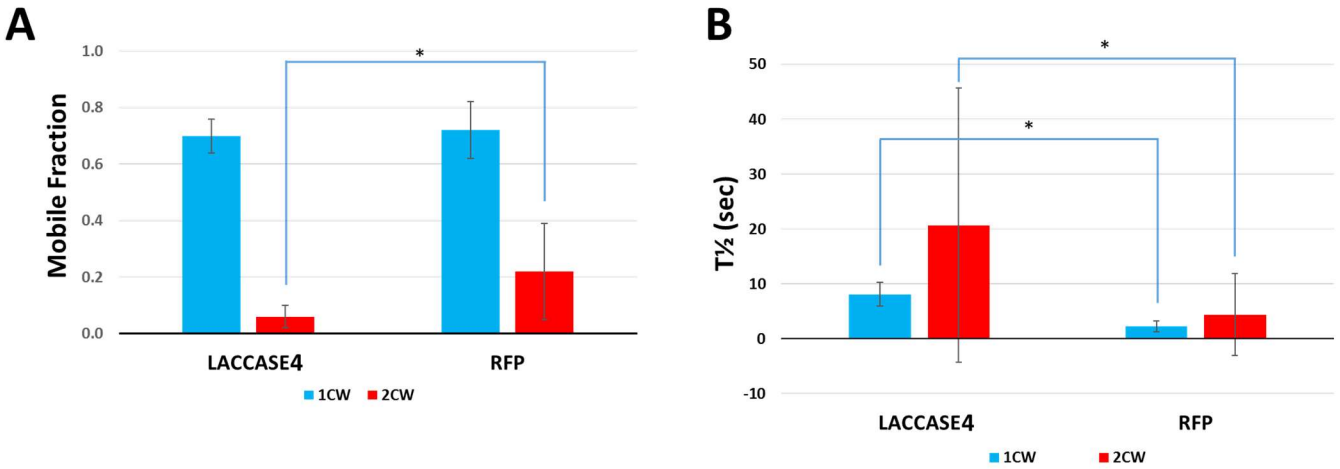

Figure 4.4: Laccases are more immobile than small fluorescent proteins in the 2CW. The average mobility (±SD) of both secreted RFP and laccases are higher in the 1CW than in the 2CW domains (A). Laccase mobility is lower than RFP mobility in the 2CW (A, Mann Whiteney U test, $p \leq 0.05$). Comparing laccase T½ to secreted RFP, in both the 1CW and 2CW laccases move less quickly (B, lower T½, $p \leq 0.05$).

4.2.3 Determining the mobility of secondary cell wall laccases in cellulose-pattern-disrupted mutants (*baculites-like1*)

Since laccases were found to be relatively immobile in the 2CW domains of protoxylem TEs compared to in the 1CW, the different composition or organization of the components that make up the 2CW compared to the 1CW could be hindering protein mobility. Cellulose is one of the three main components that make up the 2CW and while it is also present in the 1CW, the 1CW cellulose is less abundant and less ordered than the 2CW cellulose (Cooper, 2000). One hypothesis for the change in laccases mobility could be because of the differences in cellulose amount or organization between the two different cell wall environments.

To test this hypothesis, the cellulose disorganized mutant *cesa7*$^{baculites\text{-}like1}$ (Takanaka *et al., New Phytologist*, in revision) were transformed with the *proLAC4:LAC4-mCHERRY* construct in the *VND7-GR* background. In *cesa7*$^{baculites\text{-}like1}$, increased glucan levels are still found following ectopic protoxylem TE formation, however the cellulose is found evenly distributed across the cell surface, rather than in the spiral 2CW pattern. Interestingly, the microtubule array that defines the 2CW pattern and the xylan, LAC4, and lignin are still deposited into the typical bands of the spiral wall pattern. Wild-type and mutant Arabidopsis seedlings were induced to form ectopic protoxylem TEs, and the differentiated cells expressing RFP-tagged LAC4 were imaged using the FRAP technique to measure protein mobility. Similar to control wild-type ectopic protoxylem TE samples, RFP-tagged LAC4 fluorescence in *baculites'* protoxylem TE 2CW did not recover post-bleach (figure 4.5A). Both the recovered fluorescence intensity (figure 4.5C, $F_m = 0.14 \pm 0.09$) and the T½ (figure 4.5C, T½ = 27.6 ± 34.5) were reminiscent of the LAC4-

mCherry recovered fluorescence intensity and T½ (figure 4.2D; F_m = 0.22 ± 0.17, T½ = 20.7 ± 25.0), suggesting cellulose is not influencing LAC4 mobility in the 2CW.

Since *cesa7*$^{baculites\text{-}like1}$ (Takanaka *et al., New Phytologist*, in revision) is a cellulose disorganized mutant rather than a cellulose deficient mutant, one reason for the absence of laccase mobility change in *cesa7*$^{baculites\text{-}like1}$ could be due to the continued cellulose presence in the 2CW. To ascertain what happens to laccase mobility in the 2CW with reduced cellulose, seedlings were treated with a cellulose inhibiting drug, 2,6-dichlorobenzonitrile (*DCB*) (Meyer *et al.,* 1978). Arabidopsis seedlings containing both the *proLAC4:LAC4-mCHERRY* and *VND7-GR* construct were treated with 10 µM DCB for 36 h. FRAP was conducted on ectopic protoxylem TE cells and the fluorescence of RFP tagged laccase was tracked post-bleach for 60 secs (figure 4.5B). The fluorescence of the RFP tagged laccase in DCB treated seedlings still did not recover following DCB treatment (figure 4.5D; F_m = 0.09 ± 0.06, T½ = 15.4 ± 19.1), suggesting laccases are immobile even when 2CW cellulose is reduced. The pattern of laccase immobility was similar in both the *cesa7*$^{baculites\text{-}like1}$ cellulose mutants (figure 4.5C; F_m = 0.14 ± 0.09, T½ = 27.6 ± 34.5) as well as the 2CW of protoxylem TEs (figure 4.2D; F_m = 0.22 ± 0.17, T½ = 20.7 ± 25.0).

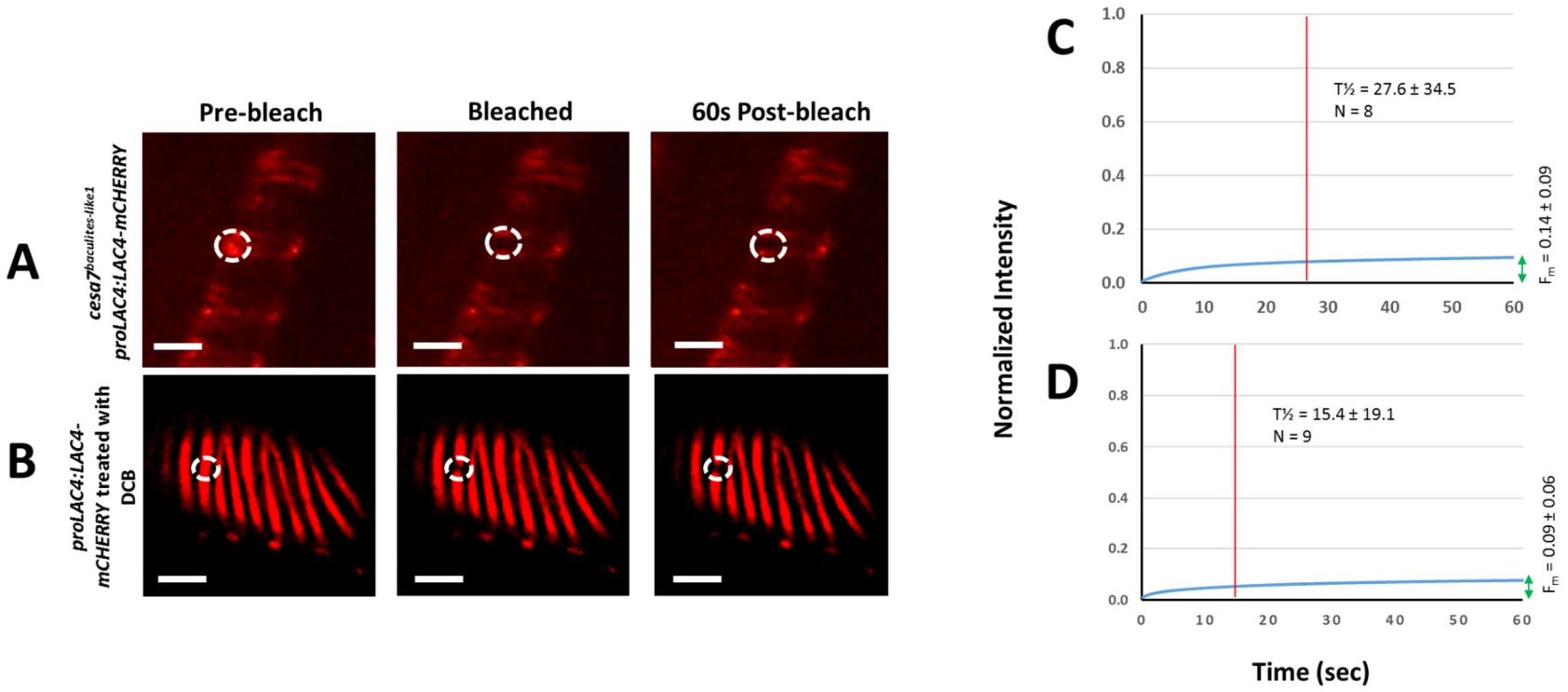

Figure 4.5: Disruption/absence of 2CW cellulose does not increase the mobility of laccases. FRAP images taken of Arabidopsis seedling apical hook cells containing (A) *cesa7*$^{baculites\text{-}like1}$ mutants transformed with *proLAC4:LAC4-mCherry/VND7-GR* (cellulose disorganized mutant), or (B) *proLAC4:LAC4-mCherry/VND7-GR* seedlings treated with DCB (cellulose inhibiting drug) before bleaching. The ROI is shown as white dashed circle at the time of bleaching and 60 secs after bleaching. All images were taken 36 h after protoxylem TE differentiation. The mobile fraction (Fm) and T½ (represented by a red line on the curves) were calculated for all FRAP experiments done (C and D). Scale bar = 3 µm.

4.2.4 Determining the mobility of secondary cell wall laccases in xylan-deficient mutants (*irx10/10-L*)

Since cellulose disorganization and absence did not increase laccase mobility in 2CW domains, the next 2CW component that I tested was the 2CW hemicellulose, glucuronoxylan, which is the major hemicellulose in dicots (Scheller and Ulvskov, 2010). Several different models have been proposed for how the components of the cell wall interact with each other through covalent or non-covalent interactions (Tan *et al.,* 2013; Busse-Wicher *et al.* 2014). In Arabidopsis, 1CW arabinoxylan (a hemicellulose) was found to be covalently crosslinked with the protein arabinogalactan (Tan *et al.,* 2013). Schuetz (2016, unpublished) also saw that 2CW xylan and laccase after oryzalin treatment on protoxylem TEs could be found co-localized despite a loss of usual 2CW banding. These findings suggest proteins and polysaccharides are tightly associated either during their secretion to the cell wall or post-secretion at the cell wall.

To test if laccase immobility in the 2CW is due to its interaction with xylan, the *proLAC4:LAC4-mCHERRY* construct was transformed into a xylan deficient double mutant *irregular xylem 10/ irregular xylem10-like* (*irx10/10-L*; Brown *et al.,* 2009) in the *VND7-GR* background. FRAP was conducted on *irx10/irx10-L* mutant Arabidopsis seedlings after ectopic protoxylem TE formation, and the mobility of RFP tagged laccases were tracked over the course of 60 secs (figure 4.6A). The fluorescence of RFP tagged laccase in the *irx10/10-L* mutants did not recover over these 60 secs (figure 4.6A). The average fluorescence recovered intensity of RFP tagged laccase in the xylan deficient background (figure 4.6D, F_m = 0.04 ± 0.03) was very similar to what was seen in the wildtype background (figure 4.1D). The averaged calculated T½ (figure 4.6D, T½ = 14.8 ± 21.2) was also similar to the wildtype (figure 4.1D). This data shows

laccase is immobile in the 2CW of the *irx10/10-L* xylan deficient mutant and suggests xylan does not constrain laccases to the 2CW.

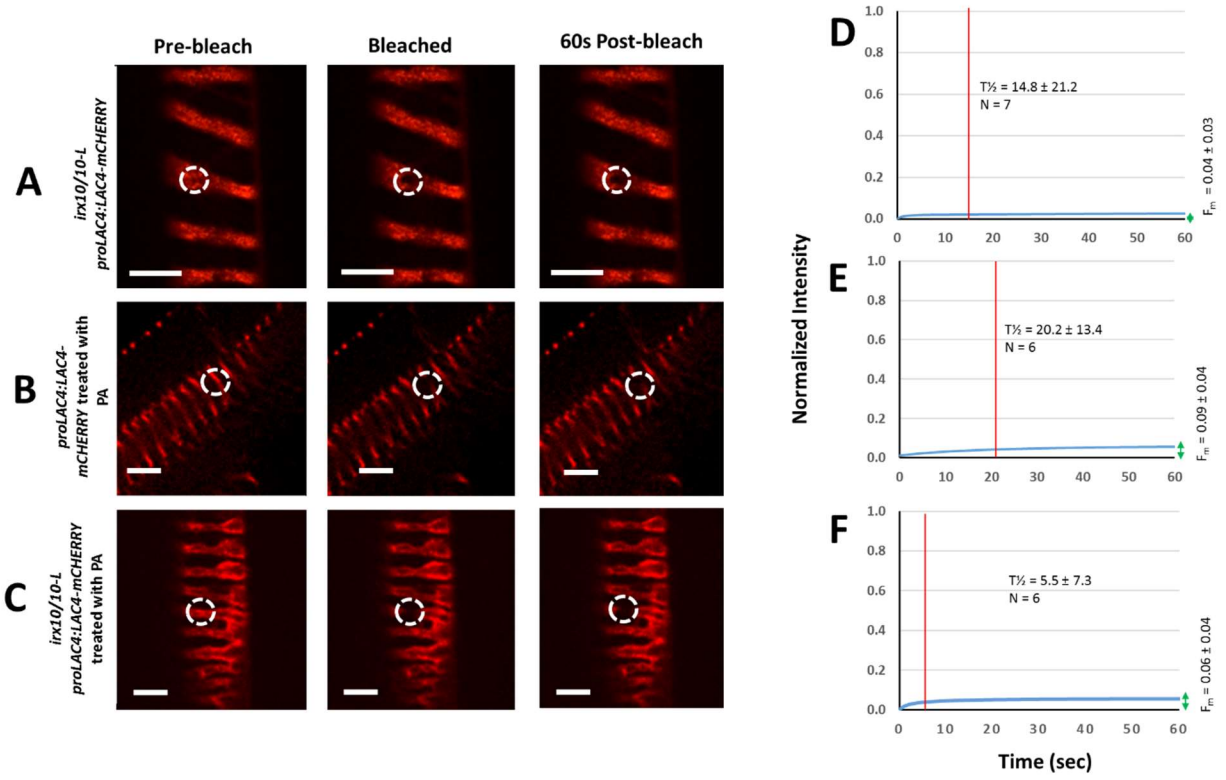

Figure 4.6: Absence of 2CW xylan and lignin does not increase the mobility of laccases. FRAP images taken of Arabidopsis seedling apical hook cells in (A) *irx10/irx10-L* mutants transformed with *proLAC4:LAC4-mCherry/VND7-GR* (xylan deficient mutant), (B) *proLAC4:LAC4-mCherry/VND7-GR* treated with PA (lignin inhibiting drug), or (C)) *irx10/irx10-L* mutants transformed with *proLAC4:LAC4-mCherry/VND7-GR* and treated with PA. Cells were bleached at the ROI (white dashed circle), and monitored over 60 secs after bleaching. All images were taken 36 h after protoxylem TE differentiation. The mobile fraction (Fm) and T½ (represented by a red line on the curves) were calculated for all FRAP experiments done (D-F). Scale bar = 3 µm.

4.2.5 Determining the mobility of secondary cell wall laccases in lignin inhibited seedlings

Absence of both cellulose and xylan did not increase laccase mobility in the 2CW, suggesting neither are the sole component involved in the constraint of laccase to the 2CW domains. The third main component of the 2CW, lignin, is a complex biopolymer which is polymerized due to oxidation of monolignols by laccases and/or peroxidases (Vanholme *et al.,* 2010). Lignin biosynthesis occurs after the cell wall polysaccharides have been laid down (Boerjan *et al.,* 2003). Since laccases are involved in polymerization of lignin, the laccases could become immobilized during the lignification process of the 2CW.

This hypothesis was tested using a lignin inhibiting drug, piperonylic acid (PA) (Kaneda *et al.,* 2008; Chong *et al.,* 2001). Arabidopsis seedlings transformed with the construct *proLAC4:LAC4-mCHERRY* in the *VND7-GR* background were treated with 10 µM of PA to elucidate the mobility of laccases when lignin is reduced. Before doing the FRAP, I tested that PA treatment successfully inhibited lignin deposition, using WT Arabidopsis seedlings treated with 10 µM PA for 48 h. The lignin deposition pattern of PA treated seedlings were compared to non-PA treated seedlings (figure 4.7). A lignin autofluorescence enhancer stain (Basic Fuchsin) was used to infer lignin presence. The fluorescence of untreated seedlings is absent from the root procambium to the root cap while the fluorescence of seedlings treated with PA were absent beyond the procambium region (figure 4.7, dashed lines). This suggests in PA treated seedlings, lignin deposition is inhibited in the native root xylem protoxylem tracheary elements due to PA treatment, and PA is an appropriate inhibitor for my further experiments.

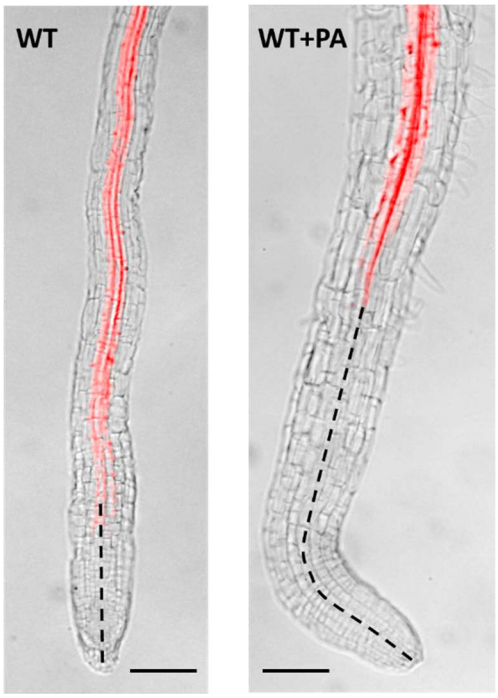

Figure 4.7: PA treatment inhibits lignin deposition in the native protoxylem TEs. WT Arabidopsis seedlings treated with or without PA for 36 h were stained with a lignin fluorescent stain (Basic Fuchsin, fluorescence depicted in red in images). Brightfield images of seedlings roots were overlaid with the Basic Fuchsin fluorescence images. The area of the root lacking lignin deposition is depicted with dashed black lines. The fluorescence in WT is absent from the procambium region to the root cap. This area is extended beyond the procambium, showing lignin deposition is inhibited upon PA treatment. Scale bar=13 µm

Once PA was ascertained to inhibit lignin, FRAP was conducted on ectopic protoxylem TEs and the mobility of RFP tagged laccases post-bleach was tracked over 60 secs (figure 4.6B). In PA treated seedlings, laccase fluorescence did not recover in the ROI during the 60 sec interval. The recovered fluorescence intensity of RFP tagged laccases in the 2CW of PA treated protoxylem TEs (figure 4.6E, F_m = 0.09 ± 0.04) was similar to the recovered fluorescence intensity of RFP tagged laccases in the 2CW of untreated protoxylem TEs (figure 4.1D). The averaged calculated T½ (figure 4.6E, T½ = 20.2 ± 13.4) of RFP tagged laccases in the 2CW was also found to be similar in treated or untreated protoxylem TEs (figure 4.2D). The consistency of the FRAP experiments between lignin-inhibited and control samples suggests lignin is not constraining laccases to the 2CW domain. Since absence of any one of the major 2CW components (cellulose, xylan and lignin) alone did not increase laccase mobility (figure 4.8A), the reason that LAC4 is constrained in the 2CW could either be its interaction with a minor, unidentified 2CW component, or the combination of the three major components. Much like a

mutant may not have a visible phenotype due to genetic redundancy, the constraint of laccase to the 2CW may be due to the contributions of multiple redundant tethering components.

To test if a combination of multiple components of the 2CW are involved in constraining laccase mobility in the 2CW, xylan deficient mutants (*irx10/irx10-L*) transformed with both the *proLAC4:LAC4*-mCHERRY and *VND7-GR* constructs were treated with 10 µM PA to inhibit lignin formation in xylan deficient mutants. FRAP was conducted on these xylan/lignin deficient protoxylem TE cells and the migration of RFP tagged laccase into the ROI was tracked for 60 secs. The fluorescence of RFP tagged laccase in the ROI of xylan/lignin deficient protoxylem cells did not visibly recover (figure 4.6C), suggesting laccases are immobile in the 2CW even with the absence of lignin and xylan. The curve of fluorescence recovery generated for the xylan/lignin deficient protoxylem TE FRAP had a calculated F_m of 0.06 ± 0.04 (figure 4.6F). This is comparable to the recovered fluorescence of RFP tagged laccases in xylan deficient mutants (figure 4.6D; F_m of 0.04 ± 0.03), lignin inhibited seedlings (figure 4.6E; F_m of 0.09 ± 0.04) and the 2CW of protoxylem TEs without treatment (figure 4.2D; F_m of 0.06 ± 0.04). The similarity between the mobility of RFP laccase in the 2CW protoxylem TE of untreated WT cells and *irx10/irx10-L* PA treated protoxylem TE cells (figure 4.8B) suggests xylan and lignin together are not components responsible for constraining laccase to the 2CW.

Despite the mobile fraction of RFP tagged laccases not changing in the absence of xylan and lignin, the half time of fluorescence recovery (T½) of RFP tagged laccase was faster in *irx10/irx10-L* PA treated protoxylem TE cells (figure 4.6F; T½ = 5.5 ± 7.3), compared to the T½ of RFP tagged laccase in the 2CW of wild-type protoxylem cells (figure 4.2D; T½ = 20.7 ± 25.0). The T½ in *irx10/irx10-L* PA treated protoxylem TE cells was comparable to the T½ of RFP tagged

laccase in the 1CW (figure 4.2C; T½ = 8.1 ± 2.2). This faster half time of fluorescence recovery is not seen when comparing all other drug or mutant FRAP experiments (figure 4.8C), suggesting that while there was not a large increase in laccase mobility, the small of number of laccases that did migrate into the ROI were able to do so more quickly in the absence of xylan and lignin. This could indicate removing xylan and lignin changes some aspect of laccase restraint in the 2CW, so that the small number of laccases that are able to migrate in the 2CW do so at faster speeds.

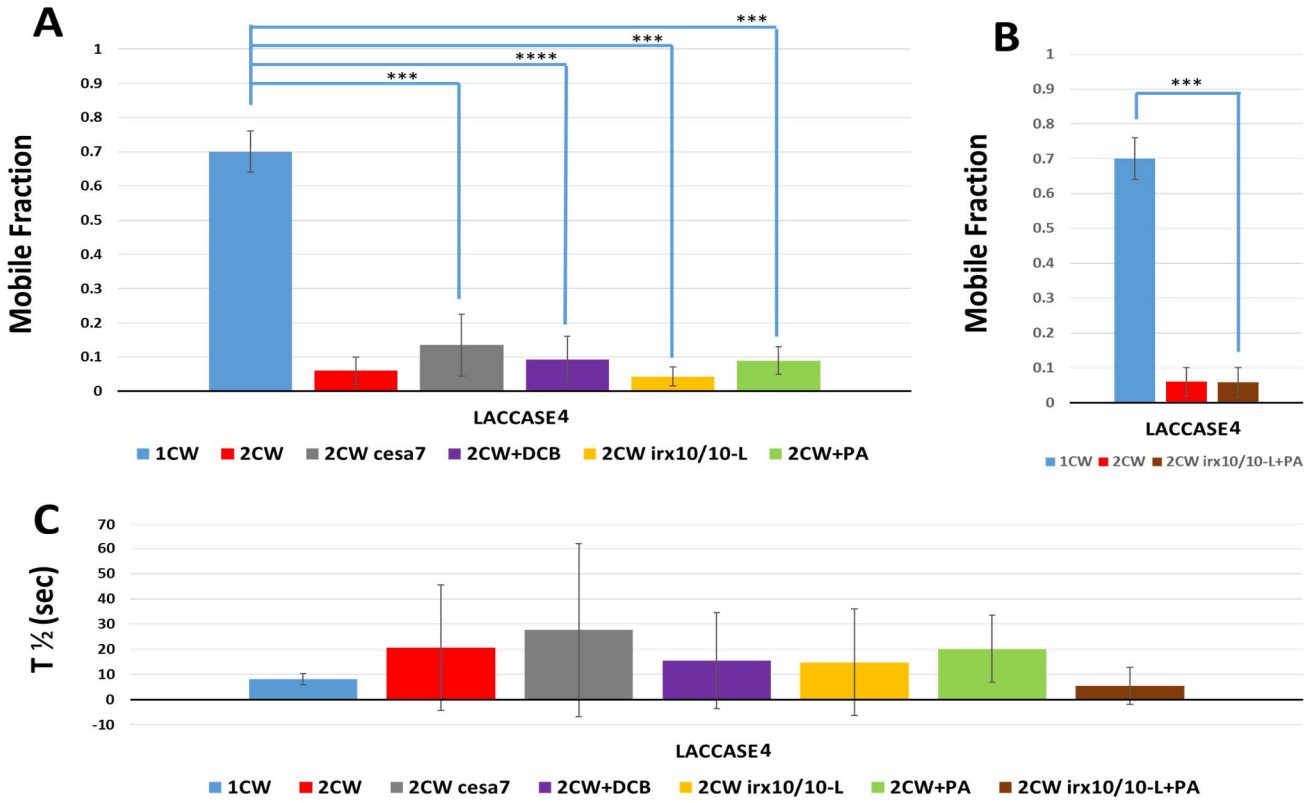

Figure 4.8: Reductions of 2CW components do not increase laccase mobility. The mobility (F_m) of the RFP tagged laccase in both the 1CW and 2CW was compared to the mobility of RFP tagged laccase in the 2CW of protoxylem TEs in (A) 1) *cesa7*$^{baculites\text{-}like1}$ (cellulose disorganized mutant), 2) DCB treated (cellulose inhibitor), 3) *irx10/irx10-L* (xylan deficient mutant), 4) PA treated and (B) 5) *irx10/irx10-L* treated with PA (xylan/lignin deficient) seedlings using the Mann Whiteney U statistical test of significance. The F_m of RFP tagged laccase is was also included but not compared using statistical tests in this figure. The F_m of all comparisons were found to be significantly different from laccase mobility in the 1CW but not the 2CW, suggesting no increase in laccase mobility regardless of cellulose, xylan nor lignin absence. (Mann Whitney U test, *** = P ≤ 0.001, **** = P ≤ 0.0001). The half time of fluorescence recovery (T½) of RFP tagged laccase in both the 1CW and 2CW was compared to the mobility of RFP tagged laccase in the 2CW of protoxylem TE in 1) *cesa7*$^{baculites\text{-}like1}$ (cellulose disorganized mutant), 2) DCB treated (cellulose inhibitor), 3) *irx10/irx10-L* (xylan deficient mutant), 4) PA treated and 5) *irx10/irx10-L* treated with PA (xylan/lignin deficient) seedlings using the Mann Whiteney U statistical test of significance (C). None of the comparisons made were found to be significantly different. Error bars = SD.

To test if the lack of mobility of laccases in lignin-deficient 2CWs is specific to laccase, or if it is true of all proteins, plant lines containing the small secreted RFP (*proUBQ10:sec-mCHERRY*) in the *VND7-GR* background were treated with 10 µM PA and imaged. FRAP was conducted on PA treated protoxylem TEs and the mobility of the secreted RFP tracked over 60 secs post-bleach (figure 4.9A). During the FRAP experiment, in protoxylem TEs treated with PA, the fluorescence of the secreted RFP in the ROI recovered through lateral diffusion. The recovered fluorescence intensity (figure 4.9B, $F_m = 0.63 \pm 0.16$) was found to be higher than the fluorescence recovery of secreted RFP in the 2CW of untreated protoxylem TEs (figure 4.1D; $F_m = 0.22 \pm 0.17$). While lateral diffusion of secreted RFP occurs in the 2CW of PA treated protoxylem TEs, the speed of fluorescence recovery is not as high as secreted RFP in the 1CW (figure 4.1C; $F_m = 0.72 \pm 0.10$) suggesting other factors are involved in constraining the secreted protein. Though not significantly different, the average T½ (figure 4.9B, T½ = 1.67 ± 1.66) of the secreted RFP in the 2CW of PA-treated protoxylem TEs was faster than the T½ of untreated protoxylem TEs (figure 4.1D; T½ = 4.4 ± 7.5), and was comparable to the T½ of secreted RFP in 1CW (figure 4.9D and 4.1C; T½ = 2.3 ± 1.0). All of this suggests that lignin imposes constraints on the mobility of proteins in the secondary cell wall generally, as seen by the increased mobility and faster half-time of recovery of the secRFP, as well as the faster half-time of recovery of LAC4. However, the stubbornly immobile fraction of LAC4 in the secondary cell wall is apparently anchored by multiple wall components.

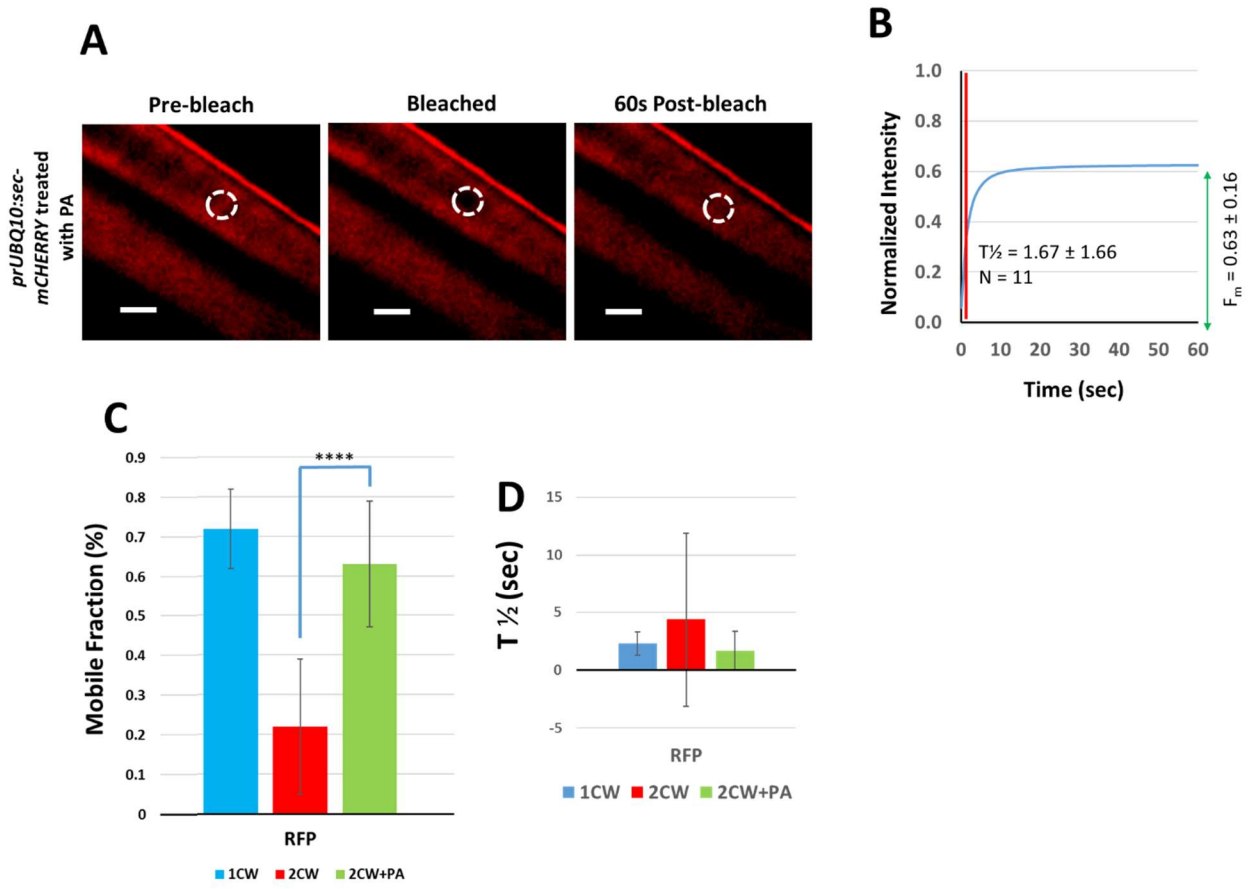

Figure 4.9: Small fluorescent proteins become more mobile in the 2CW when lignin production is inhibited. FRAP images taken of Arabidopsis seedling apical hook cells containing (A) *proUBQ10:sec-mCherry/VND7-GR.* Seedlings were treated with the lignin inhibiting drug PA for 6 h before being induced to differentiate into protoxylem TEs (for 36 h). FRAP images were taken before bleaching the ROI (white dashed circles), and fluorescence monitored post-bleach during the 60 sec experiment (A). The region bleached corresponds to the 2CW bands of the protoxylem TE cell. The mobile fraction (Fm, green double arrows) and T½ were calculated for FRAP experiment (B). An increase in protein mobility occurs when comparing the mobility of secreted mCherry in the 2CW without PA treatment to secreted mCherry in the 2CW with PA treatment (C). The mobility (F_m) of secreted mCherry in the 2CW without PA treatment was found to statistically increase (Mann Whitney U test, $P \leq 0.0001$) when compared to the mobility of secreted mCherry in the 2CW with PA treatment. Despite the difference in mean F_m, the half time of fluorescence recovery (T½) of secreted mCherry was not found to statistically different (Mann Whitney U test) among treatments. Scale bar = 3 µm. Error bars = SD.

4.3 Discussion

Laccases are required for lignin deposition in the spiral 2CWs of protoxylem TEs. While it is known that laccases localize to 2CW specific domains in protoxylem TEs, it is unknown how the laccases are anchored or contained within these domains. Previous studies looking at plasma membrane protein lateral diffusion identified the 1CW as the greatest obstacle to protein mobility (Martinière *et al*., 2013). While plasma membrane protein lateral diffusion is slowed by cell wall corralling, it is unknown if the lateral diffusion of secreted proteins within the cell wall itself has hindered mobility. Fluorescently tagged laccases and secreted RFP mobility measured using FRAP allowed me to compare the difference the 1CW and 2CW environment had on hindering protein lateral diffusion. The absence of cell wall corralling in the 1CW versus the absence of lateral diffusion seen in the 2CW of both laccases and secreted RFP demonstrates the helical 2CW pattern of laccases in protoxylem TEs is due to laccases being restricted to the 2CW region by the 2CW components/structure.

Laccases are heavily glycosylated proteins, with LAC4 itself having 14 predicted N-glycosylation sites (Strong and Claus 2011; Turlapati *et al.*, 2011), making it possible for its oligosaccharide chains to retard its movement within the polysaccharide matrix. Despite the laccase oligosaccharide tree being a possible deterrent of lateral diffusion within the 2CW, secreted RFP, which lacks glycosylation, was also immobile within the 2CW, suggesting there are other factors modulating protein mobility. Since laccases and secreted RFP freely diffuse within the 1CW but not within the 2CW, the difference in cell wall composition and structure are likely candidates for reasons this contrasting proteins mobility is seen.

What are the features of the 1CW that permit protein mobility? 1CW is deposited during cell growth, therefore it is important that the structure of the wall allow for the constant modifications needed for cell expansion. The 1CW is mainly composed of cellulose, pectin and the hemicellulose xyloglucan. Over the years there have been many models proposing how these polysaccharides are organized to form the 1CW (Carpita and Gibeaut, 1993; Tan *et al*., 2013; Cosgrove, 2014). Cell growth usually occurs on the opposite direction to the cellulose microfibrils orientation (Cosgrove, 2014; Cosgrove and Jarvis, 2012). The action of wall modifying enzymes like xyloglucan endotransglycosylases (Fry *et al.*, 1992) and wall loosening expansins then help the cell wall matrix expand between layers of microfibrils (Thomas *et al*., 2013). For enzymes like the xyloglucan endotransglycosylase to reach xyloglucan chains and modify them, a sufficient amount of space between the cellulose microfibrils must exist. One cell wall model which suggests this is coined as the "tethering network model" where xyloglucans are hypothesized to stretch between cellulose microfibrils, connecting them and allowing enough space for cell wall modifying enzymes (Cosgrove and Jarvis, 2012). Although more current models do not support the same cell wall structural organization as the tethering network model, the idea of the existence of a 'free space', which allows cell wall modifying enzymes or expansins to act, could explain why proteins such as laccases or secreted RFPs can freely diffuse within the 1CW matrix. Another model suggests the 1CW is also a strong but flexible and well hydrated structure (Dyson and Jensen, 2010). Therefore if the 1CW is fluid and organized in such a way that allows for constant expansion of the wall and is highly hydrated, there may be more 'free space' for proteins such as laccases or a secreted protein to move within its matrix.

In contrast, the 2CW is deposited after the cell was matured. Found only in special cell types, the 2CW in vascular cells is involved in strengthening the plant to allow it to stand upright against gravity as well as to resist the negative pressure of water transport through the plant vascular system (Zhong and Ye, 2015). The 2CW is composed mainly of a cellulose, lignin and xylan. In comparison to the 1CW, the 2CW is less hydrated, and more stiff. Due to deposition after cell maturation (and followed by programed cell death), the 2CW is not constantly modified by the cell like the 1CW is (Cosgrove and Jarvis, 2012). Laccases and, surprisingly, secreted RFP were both found to be immobile within the 2CW. Since both proteins were mobile in the 1CW, the cause of their immobility in the 2CW is likely due to the differences found in the organization or composition of the 2CW in comparison to the 1CW. One explanation for this difference in mobility could be due to the 2CW being less hydrated, resulting in less 'free space' than the 1CW.

The cellulose deposited in the 2CW are oriented more uniformly than in the 1CW, aligned next to one another in parallel. Although different among species, there is usually a higher percent of cellulose in the 2CW (Zhong and Ye, 2015; Barnett and Bonham, 2004). Laccases and secreted RFP were found to be immobile in 2CWs, and the close parallel and abundant nature of cellulose microfibrils could be a limiting factor to the mobility of proteins within the cell wall matrix. This restriction of laccase lateral diffusion is still present even in a variant of the *irx3* cellulose deficient mutant (Ha *et al*., 2002), *cesa7*$^{baculitse\text{-}like1}$ (Takanaka *et al*., New Phytologist, in revision). *cesa7*$^{baculites\text{-}like1}$ is a cellulose-disorganized mutant that has even cellulose deposition across both the primary and secondary cell wall of protoxylem TEs. A change in the amount and organization of cellulose in the 2CWs did not allow laccases in the

2CW to become mobile. Treatment with the cellulose inhibiting drug, DCB, also did not increase laccase mobility in the 2CW of protoxylem TEs. This suggests either cellulose organization does not play an important role in keeping laccases in the 2CW region of protoxylem TE or there are secondary factors preventing laccases from diffusing.

The major 2CW hemicellulose, glucuronoxylan, is a numerously branched polysaccharide that is synthesized in the Golgi before being secreted to the 2CW (Rennie and Scheller, 2014). Work by Tan *et al.* (2013) demonstrated that a different hemicellulose (arabinoxylan) and protein (arabinogalactan) are covalently linked in the cell wall, suggesting other hemicellulose and proteins may be capable of the same type of crosslink. However, this does not appear to be the case, given that laccases in the 2CW of xylan-deficient mutants were still constrained by the remaining 2W components. While the reason for laccases remaining immobile could be due to multiple components of the cell wall constraining its movement, laccases and xylan do not appear to be covalently crosslinked based on Co-IP data (chapter 3).

The final major component of 2CWs, lignin, is a phenolic biopolymer. A common analogy is that lignin is similar to concrete, filling in the 'extra space' found between the cellulose and hemicellulose polysaccharide matrix (Achyuthan *et al.,* 2010). Lignin not only provides the 2CW structure with strength, but also gives 2CWs the hydrophobicity needed to function in areas like the plant vasculature (Zhong and Ye, 2015). Although this property of lignin being analogous to concrete would suggest that it could be the greatest hindrance to protein mobility with the 2CW matrix, laccases did not become more mobile in lignin deficient (PA treated) 2CW environments.

Despite laccases not becoming able to diffuse in a lignin deficient 2CW matrix, secreted RFP mobility was found to increase following inhibition of lignin biosynthesis, and the increased mobility was at levels comparable to sec-RFP mobility in the 1CW. This suggests that while lignin is not the only component constraining laccases in the 2CW, it is a major component preventing lateral diffusion for other proteins. Since lignin polymerizes in between the spaces of the cell wall not filled by cellulose and hemicellulose, once lignin is inhibited, the secreted RFP is likely provided with enough space to move within the polysaccharide matrix. Laccase, however, may be constrained by its oligosaccharide chains providing steric hindrance as it moves through the polysaccharide matrix, and interacts with cellulose microfibrils or xylan.

Since each of the three major 2CW components alone were insufficient to allow laccase to freely diffuse into the neighboring cell wall space, it is likely a combination of these three components restricting its movement. Though this seemed like the logical next step in ascertaining laccase localization to protoxylem TE 2CW specific domains, removing both xylan and lignin from the 2CW were ineffective at allowing laccase lateral diffusion. While FRAP recovery curves show the mobile fraction of laccases were no different from untreated wildtype cells, the half time of recovery had a mean that was more similar to the half time of recovery seen in laccases in the 1CW. However, this difference was not statistically significant, so either it was due to random chance, or more sampling could be done to reduce the high variability.

Lignification of the spiral or helical 2CW of protoxylem tracheary elements is dependent on LAC4 and LAC17 (Schuetz *et al*., 2014). The data in this chapter demonstrates that LAC4 was immobile in the 2CW, which explains why it does not diffuse in the extracellular matrix to

regions where lignin is not deposited. My work shows that it is this immobility, rather than an exclusion zone in the 1CW, that keeps LAC4 restricted to the 2CW where it functions. The observation that ectopic LAC4 is mobile in the 1CW shows that there is no barrier to LAC4 movement in the 1CW. Two other laccases, LAC11 and LAC17 were demonstrated to be important in 2CW lignification (Zhao *et al*., 2013; Berthet *et al*., 2011). The mobility of both LAC11 and LAC17 would, therefore, be interesting to study.

Chapter 5: Conclusion and Future Directions

For my Master's thesis, I aimed to further our understanding of laccase secretion and localization to the 2CW. Laccases localized to 2CW specific domains (Schuetz *et al.*, 2014), however, the mechanisms underlying this patterning, e.g. how laccases are packaged into vesicles, the type of secretion they undergo, or how the extracellular environment constrains them in these specific domains are unknown. Therefore, my research objectives were to:

4) Ascertain if the secretion of extracellular proteins, such as laccases, changes during the formation of 2CWs.
5) Test the hypothesis that the hemicellulose xylan and laccases might be cross-linked during 2CW production.
6) Elucidate what keeps laccases restricted to 2CW-specific domains.

In chapter 3, I showed that RFP-tagged laccase was found in all regions of the primary cell wall when ectopically expressed in non-xylem cells, but it was found in 2CW specific regions after protoxylem TE differentiation. This shift in localization pattern suggests vesicle trafficking for 2CW proteins, such as laccases, changes from being nonpolar to polar during 2CW protoxylem differentiation. The same change in localization is seen for a general secreted protein, suggesting not just vesicles carrying 2CW specific proteins, but vesicles carrying many proteins are reoriented to 2CW domains during protoxylem TE differentiations. To further test this hypothesis, FRAP experiments on housekeeping proteins (such as the aquaporin PIP2) and cell wall specific proteins (such as CSC) are in progress, and FRAP will be used to identify the insertion sites of these proteins at the plasma membrane either before protoxylem

differentiation or during protoxylem differentiation. If vesicle trafficking is rerouted during protoxylem differentiation, then both proteins would insert only into the plasma membrane regions associated with the 2CW during protoxylem differentiation.

Neither laccases nor a secreted RFP were found to accumulate in the Golgi, suggesting secretion of the proteins to be transient and easily missed or, though less likely, a non-canonical secretory mechanism independent of the Golgi is occurring. Attempts to use a CESA7 promoter driving a secreted fluorophore to track Golgi movement during protoxylem differentiation were unsuccessful due to the YFP being retained in the ER. Using this promoter, we had hypothesized to see YFP secreted to 2CW specific regions in the canonical helical banding pattern and accumulation of YFP in Golgi bodies and vesicles. Further screening for successful lines where YFP does not become sequestered in the ER can be done so that these lines can be used to study if laccases are secreted via the endomembrane system. These plant lines could also help us further our understanding of the vesicle trafficking patterns of proteins during the differentiation of protoxylem TE.

Xylan was not detected during laccase protein-polysaccharide pulldown assays (and *vice versa*) suggesting a cell wall model where xylan and laccases are not covalently crosslinked. Though Co-IP pulldowns demonstrated xylan and laccases are not covalently linked, it should be noted that Co-IP is not optimized for protein-polysaccharide interactions and this crosslink could be lost during the experimental process. Furthermore, if xylan and laccases are crosslinked in the cell wall, it may be difficult to detect these covalent bonds through a pulldown assay as a majority of the protein/polysaccharide would be trapped within the insoluble portion of the cell wall.

In chapter 4 the mechanism of retention of laccase to 2CW domains was examined, by quantifying mobility of RFP-tagged laccases and a secreted control RFP using FRAP. These results show protein mobility is different in the 1CW and the 2CW. Both laccases and secreted RFP are mobile in the 1CW, while they are immobile in 2CW, leading to the conclusion that the composition or structure of the 2CW is likely more restrictive than the 1CW. This supports the hypothesis that laccase localization in 2CW specific regions is due to the 2CW constraining the laccases to these regions, rather than through exclusion from the 1CW. In plants undergoing pathogen attack the 1CW of infected cells becomes lignified in a diffuse manner (Paudyal and Hyun, 2015), suggesting laccase diffusion in the 1CW is important for plant defense. While in the 2CW, laccase immobility in the 2CW suggests laccases and other 2CW matrix polysaccharides must be secreted together so that all layers of the 2CW can become lignified.

While the focus of this thesis has been on LAC4, a member of one of the enzyme families (laccases) involved in facilitating oxidative polymerization of lignin, another family of enzymes, (peroxidases), is also capable of facilitating the polymerization of monolignols to lignin (Vanholme *et al.,* 2010). Recent studies have demonstrated that peroxidases are required for the lignification of the Casparian strip and, that there is specific restriction of peroxidases to domains formed by a plant-specific protein called CASP1 (Lee *et al*., 2013). This restriction of movement of peroxidases by CASP1 proteins is reminiscent of the restricted mobility of laccases in the 2CW. Although in the case of peroxidases, there is a scaffold of proteins (CASP1) sequestering it to the Casparian strip, for laccases the 2CW environment appears to be restricting laccase mobility.

Drug and mutant FRAP experiments were conducted to identify the component of the cell wall responsible for constraining mobility of laccases. Disrupting cellulose, xylan, lignin and both xylan and lignin did not change laccase immobility within the 2CW. Treatment with a lignin inhibitor did increase the mobility of secreted RFP in the 2CW of protoxylem TEs. Taken together, this suggests a combination of 2CW components is responsible for restraining laccase to the 2CW. Ha *et al*., (2002) analyzed the cellulose deficient mutant *cesa7*^{irx3} with NMR and FTIR, and concluded that "cellulose microfibrils … scaffold the organization of the other polymers into a coherent secondary cell wall." It is possible that loss or disorganization of cellulose led to an abnormally collapsed xylan-lignin network that constrained laccase mobility. Loss of lignin and/or xylan did not remove the abundant cellulose microfibrils, so in that case mobility was again constrained. Since secreted RFP mobility was recovered in lignin deficient 2CWs, lignin could be the component physically preventing the mobility of small proteins in the 2CW by simply filling in any excess space, while other polysaccharides in the 2CW could be restricting other protein mobility (such as laccases) through steric hindrance.

All experiments were done on one of three laccases which have been shown to be important in 2CW lignification (LAC4). Further studies could be done on the other two (LAC11 and LAC17) to see how similar to different results are would be and further our insight into how 2CW proteins are trafficked to the 2CW domains and how the laccases are restricted to these specific domains.

The objectives of my thesis have been to elucidate the secretion and localization of laccases. Vesicle trafficking of laccase and a generic secreted protein was found to shift from diffuse to targeted when cells changed from making 1CW (pre-differentiation) to making 2CW

(during protoxylem differentiation). While I was not able to track laccases in Golgi to ascertain if laccases are secreted through the endomembrane system, future work can be done to explore this hypothesis. Using FRAP techniques I was also able demonstrate laccases (as well as generic proteins) are constrained in 2CW domains while being free to diffuse in the 1CW. The difference found between the mobility of laccases in these two cell wall environments could be due to the difference in cell wall organization and/or composition. Drug and mutant studies causing cellulose, xylan, lignin and xylan/lignin disorganization or absence revealed laccases are not bound to the 2CW by a single 2CW component. Abolishing both xylan and lignin allows small generic proteins to become able to diffuse within the 2CW (like in the 1CW) but not laccases, suggesting that while cellulose along cannot restrict laccase movement, it still plays an important role in sequestering laccases to the 2CW. Combined, this thesis furthers our insight on how laccases are trafficked to 2CW specific regions and how they are retained in these special domains. This work helps us to understand the mechanism of directed lignification during development of the plant vascular system. This is important not only for understanding plant development, but also because lignin is a phenolic biopolymer with many uses in a vast number of industries (biofuel, carbon fiber, construction).

Bibliography

Achyuthan, K. E., Achyuthan, A. M., Adams, P. D., Dirk, S. M., Harper, J. C., Simmons, B. A., and Singh, A. K. (2010). Supramolecular self-assembled chaos: Polyphenolic lignin's barrier to cost-effective lignocellulosic biofuels. *Molecules, 15*(12), 8641-88. doi: 10.3390/molecules15118641.

Albersheim, P., Darvill, A., Roberts, K., Sederoff, R., and Staehelin A. (2010). *Plant cell walls: From chemistry to biology*. New York: Garland Science.

Alberts B., Johnson, A., Lewis, J., Morgan, D., Raff, M., Roberts, K., and Walter, P. (2015). *Molecular biology of the cell 6th edition*. Garland science p741-744.

Aoyama, T., and Chua, N. H. (1997). A glucocorticoid-mediated transcriptional induction system in transgenic plants. *The Plant Journal, 11*(3), 605-12. doi: 10.1046/j.1365-313X.1997.11030605.x.

Barnett, J. R., and Bonham V. A. (2004). Cellulose microfibril angle in the cell wall of wood fibres. *Biol. Rev., 79,* 461–472. doi: 10.1017/S1464793103006377.

Berthet, S., Demont-Caulet, N., Pollet, B., Bidzinski, P., Cézard, L., Le Bris, P., … Jouanin, L. (2011). Disruption of LACCASE4 and 17 results in tissue-specific alterations to lignification of Arabidopsis thaliana stems. *The Plant Cell, 23*(3), 1124–1137. doi: 10.1105/tpc.110.082792

Boerjan, W., Ralph, J., and Baucher, M. (2003). Lignin Biosynthesis. *Ann. Rev. Plant Biol., 54,* 519–549. doi: 10.1146/annurev.arplant.54.031902.134938.

Brown, D. M., Goubet, F., Wong, V. W., Goodacre, R., Stephens, E., Dupree, P. and Turner, S. R. (2007). Comparison of five xylan synthesis mutants reveals new insight into the mechanisms of xylan synthesis. *The Plant Journal, 52,* 1154–1168. doi: 10.1111/j.1365-313X.2007.03307.x.

Brown, D. M., Zhang, Z., Stephens, E., Dupree, P., and Turner, S. R. (2009). Characterization of IRX10 and IRX10-like reveals an essential role in glucuronoxylan biosynthesis in Arabidopsis. *The Plant Journal, 57,* 732–746. doi: 10.1111/j.1365-313X.2008.03729.x.

Busse-Wicher, M., Li, A., Silveira, R. L., Pereira, C. S., Tryfona, T., Gomes, T. C., Skaf, M. S., and Dupree, P. (2016). Evolution of xylan substitution patterns in gymnosperms and angiosperms: Implications for xylan interaction with cellulose. *Plant Physiology 171*(4), 2418-31. doi: 10.1104/pp.16.00539.

Carpita, N. C., and Gibeaut, D. M. (1993). Structural models of primary cell walls in flowering plants: Consistency of molecular structure with the physical properties of the walls during growth. *The Plant Journal, 3*(1), 1-30. doi: 10.1111/j.1365-313X.1993.tb00007.x.

Chong, J., Pierrel, M. A., Atanassova, R., Werck-Reichhart, D., Fritig, B., and Saindrenan, P. (2001). Free and conjugated benzoic acid in tobacco plants and cell cultures. Induced accumulation upon elicitation of defense responses and role as salicylic acid precursors. *Plant Physiology, 125*(1), 318-28. doi: http://dx.doi.org/10.1104/pp.125.1.318

Clough, S. J., and Bent, A. F. (1998). Floral dip: A simplified method for Agrobacterium-mediated transformation of Arabidopsis thaliana. *The Plant Journal, 16*(6), 735-43. doi: 10.1046/j.1365-313x.1998.00343.x

Cooper G. M. (2000). *The Cell: A Molecular Approach. 2nd edition*. Sunderland (MA), Sinauer Associates. Cell Walls and the Extracellular Matrix. Available from: https://www.ncbi.nlm.nih.gov/books/NBK9874/

Cosgrove D., and Jarvis M. (2012). Comparative structure and biomechanics of plant primary and secondary cell walls. *Front Plant Sci. 3*, 204. doi: 10.3389/fpls.2012.00204

Cosgrove, D. (2005). Growth of the plant cell wall. *Nature Reviews Molecular Cell Biology, 6*, 8 50-861. doi: 10.1038/nrm1746.

Cosgrove, D. (2014). Re-constructing our models of cellulose and primary cell wall assembly. *Current Opinion in Plant Biology, 22*, 122–131. http://doi.org/10.1016/j.pbi.2014.11.001.

DeBono, A., Yeats, T. H., Rose, J. K. C., Bird, D., Jetter, R., Kunst, L., and Samuels, L. (2009). Arabidopsis LTPG is a glycosylphosphatidylinositol-anchored lipid transfer protein required for export of lipids to the plant surface. *The Plant Cell, 21*(4), 1230–1238. doi: 10.1105/tpc.108.064451.

Demura, T., Tashiro, G., Horiguchi, G., Kishimoto, N., Kubo, M., Matsuoka, N., … Fukuda, H. (2002). Visualization by comprehensive microarray analysis of gene expression programs during transdifferentiation of mesophyll cells into xylem cells. *PNAS, 99*(24), 15794–15799. http://doi.org/10.1073/pnas.232590499.

Dharmawardhana, D. P., Ellis, B. E., and Carlson J. E. (1992). Characterization of vascular lignification in Arabidopsis thaliana. *Can. J. Bot.*, 70, 2238-2244. doi: 10.1139/b92-277.

Driouich, A., Lainé, A.-C., Vian, B. and Faye, L. (1992), Characterization and localization of laccase forms in stem and cell cultures of sycamore. *The Plant Journal, 2*, 13–24. doi:10.1111/j.1365-313X.1992.00013.x.

Dyson, R. Y., and Jensen O. E. (2010). A fibre-reinforced fluid model of anisotropic plant cell growth. *J. Fluid Mech., 655*, 472–503. doi: 10.1017/S002211201000100X.

Feraru, E., and Friml, J. (2008). PIN Polar Targeting. *Plant Physiology, 147*(4), 1553–1559. http://doi.org/10.1104/pp.108.121756

Fry, S. C., Smith, R. C., Renwick, K. F., Martin, D. J., Hodge, S. K., and Matthews, K. J. (1992). Xyloglucan endotransglycosylase, a new wall-loosening enzyme activity from plants. *Biochemical Journal, 282*(Pt 3), 821–828. doi: 10.1042/bj2820821.

Fukuda, H. (1996). Xylogenesis: Initiation, progression and cell death. *Annual Review of Plant Physiology and Plant Molecular Biology, 47*, 299–325. doi: 10.1146/annurev.arplant.47.1.299.

Gendre, D., Oh, J., Boutté, Y., Best, J. G., Samuels, L., Nilsson, R., … Bhalerao, R. P. (2011). Conserved Arabidopsis ECHIDNA protein mediates trans-Golgi-network trafficking and cell elongation. *Proc Natl Acad Sci USA., 108*(19), 8048-53. doi: 10.1073/pnas.1018371108.

Gendre, D., McFarlane, H. E., Johnson, E., Mouille, G., Sjödin, A., Oh, J., … Bhalerao, R. P. (2013). Trans-Golgi network localized ECHIDNA/Ypt interacting protein complex is required for the secretion of cell wall polysaccharides in Arabidopsis. *The Plant Cell, 25*, 2633–46. doi: 10.1105/tpc.113.112482.

Ha, M. A., MacKinnon, I. M., Sturcová, A., Apperley, D. C., McCann, M. C., Turner, S. R., and Jarvis, M. C. (2002). Structure of cellulose-deficient secondary cell walls from the irx3 mutant of Arabidopsis thaliana. *Phytochemistry, 61*(1), 7-14.

Hayashi, R., Wada, H., Ito, K., and Adcock, I. M. (2004). Effects of glucocorticoids on gene transcription. *European Journal of Pharmacology, 500*(1-3), 51-62. doi: 10.1016/j.ejphar.2004.07.011.

Hepler, PK. and Newcomb, EH. (1964). Microtubules and fibrils in the cytoplasm of coleus cells undergoing secondary cell wall deposition. *Cell Biol., 20,* 529-32. doi: 10.1083/jcb.20.3.529.

Kaneda, M., Rensing, K. H., Wong, J. C., Banno, B., Mansfield, S. D., and Samuels, A. L. (2008). Tracking monolignols during wood development in lodgepole pine. *Plant Physiology, 147*(4), 1750-60. doi: 10.1104/pp.108.121533.

Kim, S.-J., and Brandizzi, F. (2016). The plant secretory pathway for the trafficking of cell wall polysaccharides and glycoproteins. *Glycobiology, 26*(9), 940-949. doi: 10.1093/glycob/cww044.

Kuang B., Zhao X., Zhou C., Zeng W., Ren J., Ebert B., ... Wu A.-M. Role of UDP-Glucuronic Acid Decarboxylase in Xylan Biosynthesis in Arabidopsis. *Molecular Plant, 9*(8), 1119-1131. doi: 10.1016/j.molp.2016.04.013.

Kubo M., Udagawa M., Nishikubo N., Horiguchi G., Yamaguchi M., Ito J. … Demura, T. (2005). Transcription switches for protoxylem and metaxylem vessel formation. *Genes Dev., 19*, 1855–1860. doi: 10.1101/gad.1331305 .

Kubo, M., Udagawa, M., Nishikubo, N., Horiguchi, G., Yamaguchi, M., Ito, J., … Demura, T. (2005). Transcription switches for protoxylem and metaxylem vessel formation. *Genes and Development, 19*(16), 1855–1860. doi: 10.1101/gad.1331305.

Lauber, M. H., Waizenegger, I., Steinmann, T., Schwarz, H., Mayer, U., Hwang, I., … Jürgens, G. (1997). The Arabidopsis KNOLLE protein is a cytokinesis-specific syntaxin. *J. Cell Biol., 139*, 1485 -1493.

Lee, C., O'Neill, M. A., Tsumuraya, Y., Darvill, A. G., and Ye, Z. H. (2007). The irregular xylem9 mutant is deficient in xylan xylosyltransferase activity. *Plant Cell Physiol., 48*, 1624–1634

Lee, Y., Rubio M., Alassimone J., and Geldner N. (2013). A Mechanism for Localized Lignin Deposition in the Endodermis. *Cell, 153*(2), 402–412. http://dx.doi.org/10.1016/j.cell.2013.02.045.

Li, S., van Os, G. M. A., Ren, S., Yu, D., Ketelaar, T., Emons, A. M. C., and Liu, C.-M. (2010). Expression and Functional Analyses of EXO70 Genes in Arabidopsis Implicate Their Roles in Regulating Cell Type-Specific Exocytosis. *Plant Physiology, 154*(4), 1819–1830. http://doi.org/10.1104/pp.110.164178.

Liepman, A. H., Wightman, R., Geshi, N., Turner, S. R., & Scheller, H. V. (2010). Arabidopsis - A powerful model system for plant cell wall research. *Plant Journal, 61*(6), 1107–1121. doi: 10.1111/j.1365-313X.2010.04161.x.

Liu, C. J., Miao, Y. C., and Zhang, K. W. (2011). Sequestration and transport of lignin monomeric precursors. *Molecules, 16*(1), 710–727. doi: 10.3390/molecules16010710

Lukowitz, W., Mayer, U. and Jürgens, G. (1996). Cytokinesis in the Arabidopsis embryo involves the syntaxin-related KNOLLE gene product. *Cell, 84*, 61-71.

Marjamaa, K., Kukkola, E. M. and Fagerstedt, K. V. (2009). The role of xylem class III peroxidases in lignification. *J. Exp. Bot., 60* (2), 367-376. doi: 10.1093/jxb/ern278.

Martinière, A., and Runions, J. (2013). Protein diffusion in plant cell plasma membranes:the cell-wall corral. *Frontiers in Plant Science, 4*, 515. doi: 10.3389/fpls.2013.00515.

Martinière, A., Lavagi, I., Nageswaran, G., Rolfe, D. J., Maneta-Peyret, L., Luu, D.-T., … Runions, J. (2012). Cell wall constrains lateral diffusion of plant plasma-membrane proteins. *PNAS, 109*(31), 12805–12810. doi: 10.1073/pnas.1202040109.

McFarlane, H. E., Döring, A., and Persson, S. (2014). The cell biology of cellulose synthesis. *Annual Review of Plant Biology, 65*, 69–94. doi: 10.1146/annurev-arplant-050213-040240.

McFarlane, H. E., Watanabe, Y., Gendre, D., Carruthers, K., Levesque-Tremblay, G., Haughn, G. W., Bhalerao, R. P., Samuels, L. (2013). Cell wall polysaccharides are mislocalized to the Vacuole in echidna mutants. *Plant Cell Physiol., 54*(11), 1867-80. doi: 10.1093/pcp/pct129.

Meyer, Y. and Herth, W. (1978). Chemical inhibition of cell wall formation and cytokinesis, but not of nuclear division, in protoplasts of Nicotiana tabacum L. cultivated in vitro. *Planta, 142*, 253-262.

Nebenführ, A., Ritzenthaler, C., and Robinson, DG. (2002). Brefeldin A: Deciphering an enigmatic inhibitor of secretion. *Plant Physiology, 130*(3), 1102-8. doi: 10.1104/pp.011569.

Oda Y., and Fukuda H. (2012). Initiation of cell wall pattern by a Rho- and microtubule-driven symmetry breaking. *Science, 337*, 1333–1336. doi: 10.1126/science.1222597.

Oda, Y., and Fukuda, H. (2014). Emerging roles of small GTPases in secondary cell wall development. *Frontiers in Plant Science, 5*, 1–6. doi: 10.3389/fpls.2014.00428.

Oda, Y., Iida, Y., Nagashima, Y., Sugiyama, Y., and Fukuda, H. (2014). Novel Coiled-Coil Proteins Regulate Exocyst Association with Cortical Microtubules in Xylem Cells via the Conserved Oligomeric Golgi-Complex 2 Protein. *Plant and Cell Physiology, 56*(2), 277–286. doi: 10.1093/pcp/pcu197.

O'Malley D., Whetten R., Bao, W., Chen, C., and Sederoff R. (1993). The role of laccase in lignification. *The plant journal, 4*(5), 751-757.

Pandey, J. L., Kiemle, S. N., Richard, T. L., Zhu, Y., Cosgrove, D. J., and Anderson, C. T. (2016). Investigating Biochemical and Developmental Dependencies of Lignification with a Click-Compatible Monolignol Analog in Arabidopsis thaliana Stems. *Frontiers in Plant Science, 7*, 1309. http://doi.org/10.3389/fpls.2016.01309.

Paudyal, D. P., and Hyun, J.-W. (2015). Physical Changes in Satsuma Mandarin Leaf after Infection of *Elsinoë fawcettii* Causing Citrus Scab Disease. *The Plant Pathology Journal, 31*(4), 421–427. http://doi.org/10.5423/PPJ.NT.05.2015.0086

Pumplin, N., Zhang, X., Noar, R. D., and Harrison, M. J. (2012). Polar localization of a symbiosis-specific phosphate transporter is mediated by a transient reorientation of secretion. *PNAS, 109*(11), 665–672. doi: 10.1073/pnas.1110215109.

Ragauskas, A. J., Beckham, G. T., Biddy, M. J., Chandra, R., Chen, F., Davis, M. F., … Wyman, C. E. (2014). Lignin valorization: Improving lignin processing in the biorefinergy. *Science, 344*(6185), 1246843. doi: 10.1126/science.1246843.

Ralph, J., Lundquist, K., Brunow, G., Lu, F., Kim, H., Schatz, P., … Boergan W. (2004). Lignins: Natural polymers from oxidative coupling of 4-hydroxyphenylpropanoids. *Phytochemistry Reviews,* 3, 29. doi: 10.1023/B:PHYT.0000047809.65444.a4

Raven, P. H., Evert, R. F., and Eichhorn, S. E. (2005). *Biology of plants*. New York: W.H. Freeman and Co.

Rennie, E., and Scheller, H. V. (2014). Xylan biosynthesis. *Current Opinion in Biotechnology, 26*, 100–107. doi: 10.1016/j.copbio.2013.11.013.

Scheller, H. V., and Ulvskov, P. (2010). Hemicellulose. *Annu. Rev. Plant Biol. 61*, 263-289. doi: 10.1146/annurev-arplant-042809-112315.

Schindelin, J., Arganda-Carreras, I., Frise, E., Kaynig, V., Longair, M., Pietzsch, T., … Cardona, A. (2012). Fiji - an Open Source platform for biological image analysis. *Nature Methods, 9(7)*, 10.1038/nmeth.2019. http://doi.org/10.1038/nmeth.2019.

Schuetz, M., Benske, A., Smith, R. A., Watanabe, Y., Tobimatsu, Y., Ralph, J., … Samuels, A. L. (2014). Laccases Direct Lignification in the Discrete Secondary Cell Wall Domains of Protoxylem. *Plant Phys., 166*(2), 798–807. doi: 10.1104/pp.114.245597.

Sibout R., and Hofte H. (2012). Plant cell biology:The ABC of monolignol transport. *Curr Biol., 22*(13), R533-5. doi: 10.1016/j.cub.2012.05.005.

Sterjiades, R., Dean, J. F. D., & Eriksson, K.-E. L. (1992). Laccase from Sycamore Maple (*Acer pseudoplatanus*) Polymerizes Monolignols. *Plant Physiology, 99*(3), 1162–1168.

Strong, P. J. and Claus, H. (2011) Laccase: A Review of Its Past and Its Future in Bioremediation. *Critical Reviews in Environmental Science and Technology, 41*(4), 373-434. doi: 10.1080/10643380902945706.

Synek, L., Schlager, N., Eliáš, M., Quentin, M., Hauser, M. -T., and Žárský, V. (2006). AtEXO70A1, a member of a family of putative exocyst subunits specifically expanded in land plants, is important for polar growth and plant development. *The Plant Journal : For Cell and Molecular Biology, 48*(1), 54–72. http://doi.org/10.1111/j.1365-313X.2006.02854.x.

Tamm, L. K. (2013). Lateral membrane diffusion corralled. *Biophysical Journal, 104*(7), 1399–1400. doi: 10.1016/j.bpj.2013.02.046.

Tan, L., Eberhard, S., Pattathil, S., Warder, C., Glushka, J., Yuan, C., … Mohnen, D. (2013). An Arabidopsis Cell Wall Proteoglycan Consists of Pectin and Arabinoxylan Covalently Linked to an Arabinogalactan Protein. *The Plant Cell, 2*5(1), 270–287. http://doi.org/10.1105/tpc.112.107334.

Thomas, L. H., Forsyth, V. T., Šturcová, A., Kennedy, C. J., May, R. P., Altaner, C. M., … Jarvis, M. C. (2013). Structure of Cellulose Microfibrils in Primary Cell Walls from Collenchyma. *Plant Physiology, 161*(1), 465–476. http://doi.org/10.1104/pp.112.206359.

Turlapati, P. V., Kim, K. W., Davin, L. B., and Lewis, N. G. (2011). The laccase multigene family in Arabidopsis thaliana:Towards addressing the mystery of their gene function(s). *Planta, 233*(3), 439–470. doi: 10.1007/s00425-010-1298-3.

Turner, S., Gallois, P., and Brown, D. (2007). Tracheary element differentiation. *Annu. Rev. Plant Biol., 58*, 407–433. doi: 10.1146/annurev.arplant.57.032905.105236.

Uemura, T. (2016). Physiological Roles of Plant Post-Golgi Transport Pathways in Membrane Trafficking. *Plant Cell Physiol., 57*(10), 2013-2019.

Van Damme, D., Inzé, D., and Russinova, E. (2008). Vesicle Trafficking during Somatic Cytokinesis. *Plant Physiology, 147*(4), 1544–1552. http://doi.org/10.1104/pp.108.120303

Vanholme, R., Demedts, B., Morreel, K., Ralph, J., and Boerjan, W. (2010). Lignin biosynthesis and structure. *Plant Physiology, 153*(3), 895–905. doi: 10.1104/pp.110.155119.

Völker A., Stierhof, Y. D., Jürgens G. (2001). Cell cycle-independent expression of the Arabidopsis cytokinesis-specific syntaxin KNOLLE results in mistargeting to the plasma membrane and is not sufficient for cytokinesis. *J Cell Sci., 114*, 3001–3012.

Watanabe, T. and Kushijima, T. (1988). Evidence for an ester linkage between lignin and glucuronic acid in lignin-carbohydrate complexes by DDQ-oxidation. *Agric. Biol. Chem. 52*, 2953-2955. doi: 10.1007/BF00386018.

Watanabe, Y., Meents, M. J., McDonnell, L. M., Barkwill, S., Sampathkumar, A., Cartwright, H. N., Demura, T., Ehrhardt, D. W., Samuels, A. L., and Mansfield, S. D. (2015). Visualization of cellulose synthases in Arabidopsis secondary cell walls. *Science, 350*(6257), 198-203. doi: 10.1126/science.aac7446.

Welinder, K. G., Justesen, A. F., Kjaersgård, I. V. H., Jensen, R. B., Rasmussen, S. K., Jespersen, H. M., and Duroux, L. (2002). Structural diversity and transcription of class III peroxidases from Arabidopsis thaliana. *European Journal of Biochemistry, 269*, 6063-6081. doi: 10.1046/j.1432-1033.2002.03311.x.

Whetten, R., and Sederoff, R. (1995). Lignin Biosynthesis. *The Plant Cell, 7*(7), 1001–1013. doi: 10.1105/tpc.7.7.1001

Wightman, R. and Turner, S. R. (2008), The roles of the cytoskeleton during cellulose deposition at the secondary cell wall. *The Plant Journal, 54*, 794–805. doi: 10.1111/j.1365-313X.2008.03444.x.

Wu, A.-M., Rihouey, C., Seveno, M., Hornblad, E., Singh, S. K., Matsunaga, T., … Marchant, A. (2009). The Arabidopsis IRX10 and IRX10-LIKE glycosyltransferases are critical for glucuronoxylan biosynthesis during secondary cell wall formation. *The Plant Journal, 57*, 718–731. doi: 10.1111/j.1365-313X.2008.03724.x.

Wu, A.-M., Hornblad, E., Voxeur, A., Gerber, L., Rihouey, C., Lerouge, P., and Marchant, A. (2010). Analysis of the Arabidopsis IRX9/IRX9-L and IRX14/IRX14-L pairs of glycosyltransferase genes reveals critical contributions to biosynthesis of the hemicellulose glucuronoxylan. *Plant Physiol., 153*, 542–554. doi: 10.1104/pp.110.154971.

Yamaguchi, M., Goué, N., Igarashi, H., Ohtani, M., Nakano, Y., Mortimer, J. C., … Demura, T. (2010). VASCULAR-RELATED NAC-DOMAIN6 and VASCULAR-RELATED NAC-DOMAIN7 effectively induce transdifferentiation into xylem vessel elements under control of an induction system. *Plant Physiology, 153*, 906–914. doi: 10.1104/pp.110.154013.

Yamaguchi, M., Mitsuda, N., Ohtani, M., Ohme-Takagi, M., Kato, K. and Demura, T. (2011), VASCULAR-RELATED NAC-DOMAIN 7 directly regulates the expression of a broad range of genes for xylem vessel formation. *The Plant Journal, 66*, 579–590. doi: 10.1111/j.1365-.

Zhao, Q., Nakashima, J., Chen, F., Yin, Y. B., Fu, C. X., Yun, J. F., … Dixon, R. A. (2013). Laccase is necessary and nonredundant with peroxidase for lignin polymerization during vascular development in Arabidopsis. *The Plant Cell, 25*, 3976-3987.

Zhong, R. and Ye, Z.-H. (2015). Secondary Cell Walls:Biosynthesis, Patterned Deposition and Transcriptional Regulation. *Plant Cell Physiol., 56*(2), 195-214. doi: 10.1093/pcp/pcu140.